ATTACHMENT 5

nutech ENGINEERS

GPC-07-102
Revision A
May 1983
GPC007.0102

DESIGN REPORT
FOR
WELD OVERLAY REPAIRS
AND FLAW EVAULATIONS
IN
RECIRCULATION AND RHR SYSTEMS
AT
E. I. HATCH NUCLEAR POWER PLANT
UNIT 2

Prepared for
Georgia Power Company

Prepared by
NUTECH Engineers, Inc.
San Jose, California

Prepared by:

H. L. Gustin, P.E.
Project Engineer

Reviewed by:

P. E. Reeves
Project Quality Assurance Engineer

Approved by:

J. E. Charnley, P.E.
Unit Supervisor

Issued by:

N. Eng
Project Manager

Date: _____

nutech ENGINEERS

REVISION CONTROL SHEET

REVISION CONTROL SHEET

CERTIFICATION BY REGISTERED PROFESSIONAL ENGINEER

I hereby certify that this document and the calculations contained herein were prepared under my direct supervision, reviewed by me, and to the best of my knowledge are correct and complete. I am a duly Registered Professional Engineer under the laws of the State of California and am competent to review this document.

Certified by:

_____

J. E. Charnley

Professional Engineer
State of California
Registration No. 16340

Date _____

TABLE OF CONTENTS

TABLE OF CONTENTS
(Continued)

Page

LIST OF TABLES

LIST OF FIGURES

LIST OF FIGURES
(Continued)

1.0 INTRODUCTION

This report summarizes evaluations performed by NUTECH to assess weld overlay repairs and unrepaired flaws in the Recirculation and RHR Systems at Georgia Power Company's E. I. Hatch Nuclear Power Plant Unit 2 (Hatch 2). Weld overlay repairs have been applied to address ultrasonic (UT) examination results believed to be indicative of intergranular stress corrosion cracking (IGSCC) in the vicinity of the welds. The purpose of each overlay is to arrest any further propagation of the cracking, and to restore original design safety margins to the weld. The unrepaired welds which had UT examination indications have been shown by analysis to still have the original design safety margins.

The required design life of each weld overlay repair is at least five years. The amount that the actual life exceeds five years will be established by a combination of future analysis and testing.

UT indications have been detected adjacent to nine 28" elbow to pipe welds, eighteen 12" elbow to pipe welds, four recirculation pipe to safe-end welds, one 12" pipe to pipe weld, two 20" inch RHR pipe to elbow welds, one 24" RHR pipe to elbow weld, and four 22" end

cap to header welds. These welds were repaired with weld overlay designs evaluated in this report, with the exception of the 28", 24", and 20" welds, which were found to be acceptable without repair.

Figure 1.1 shows all the welds in relation to the Reactor Pressure Vessel and other portions of the Recirculation and RHR Systems. Table 1.1 lists the welds evaluated in this report, describes the indications found at each location, and identifies the type of repair (as defined in Section 2) performed. All of the existing affected RHR and Recirculation System materials are Type 304 stainless steel.

Weld Identification Number	Orientation	Flaw Description Maximum Depth	Maximum Length	Flaw Disposition
2B31-1RC-22AM-1	Circumferential	42%	53"	Weld overlay per Fig. 2.3
2B31-1RC-22AM-4	Circumferential	19%	60"	Weld overlay per Fig. 2.3
2B31-1RC-22BM-1	Circumferential	40%	25½"	Weld overlay per Fig. 2.3
2B31-1RC-22BM-4	Circumferential	37%	360°	Replace End Cap
2B31-1RC-28A-3	Circumferential	12%	5½"	Acceptable by analysis
2B31-1RC-28A-4	Circumferential	17%	360°	Acceptable by analysis
2B31-1RC-28A-7	Circumferential	8%	360°	Acceptable by analysis
2B31-1RC-28A-10	Circumferential	10%	1¼"	Acceptable by analysis
2B31-1RC-28B-3	Circumferential	15%	360°	Acceptable by analysis
2B31-1RC-28B-7	Circumferential	18%	360°	Acceptable by analysis
2B31-1RC-28B-8	Circumferential	7%	360°	Acceptable by analysis
2B31-1RC-28B-10	Circumferential	20%	360°	Acceptable by analysis
2B31-1RC-28B-15	Circumferential	23%	360°	Acceptable by analysis
2E11-1RHR-20RS-2	Circumferential	13%	360°	Acceptable by analysis
2E11-1RHR-20RS-3	Circumferential	14%	360°	Acceptable by analysis
2E11-1RHR-24BR-11	Circumferential	18%	10 9/16"	Acceptable by analysis

Table 1.1

Indentification of Observed UT Indications

Weld Identification Number	Orientation	Flaw Description Maximum Depth	Maximum Length	Flaw Disposition
2B31-1RC-12BR-A3	Circumferential	25%	360°	Weld overlay per Fig. 2.2
2B31-1RC-12BR-B2	Circumferential	26%	360°	Weld overlay per Fig. 2.2
2B31-1RC-12BR-B3	Circumferential	22%	360°	Weld overlay per Fig. 2.2
2B31-1RC-12BR-B4	Circumferential	23%	360°	Weld overlay per Fig. 2.2
2B31-1RC-12BR-C2	Circumferential	28%	360°	Weld overlay per Fig. 2.2
2B31-1RC-12BR-C3	Circumferential	30%	360°	Weld overlay per Fig. 2.1
2B31-1RC-12BR-C4	Circumferential	32%	360°	Weld overlay per Fig. 2.1
2B31-1RC-12BR-D2	Circumferential	14%	360°	Weld overlay per Fig. 2.2
2B31-1RC-12BR-D3	Circumferential	17%	360°	Weld overlay per Fig. 2.2
2B31-1RC-12BD-E3	Circumferential	22%	360°	Weld overlay per Fig. 2.2
2B31-1RC-12BD-E3A	Circumferential	21%	360°	Weld overlay per Fig. 2.2
2B31-1RC-12BD-E4	Circumferential	18%	360°	Weld overlay per Fig. 2.2
2B31-1RC-12AR-F2	Circumferential	25%	360°	Weld overlay per Fig. 2.2
2B31-1RC-12AR-F3	Circumferential	10%	360°	Weld overlay per Fig. 2.2
2B31-1RC-12AR-G2	Circumferential	14%	360°	Weld overlay per Fig. 2.2
2B31-1RC-12AR-G3	Circumferential	15%	360°	Weld overlay per Fig. 2.2
2B31-1RC-12AR-H2	Circumferential	10%	360°	Weld overlay per Fig. 2.2
2B31-1RC-12AR-H3	Circumferential	30%	360°	Weld overlay per Fig. 2.2
2B31-1RC-12AR-J2	Circumferential	23%	360°	Weld overlay per Fig. 2.2
2B31-1RC-12AR-J3	Circumferential	30%	360°	Weld overlay per Fig. 2.2

Weld Identification Number	Orientation	Flaw Description Maximum Depth	Maximum Length	Flaw Disposition
2B31-1RC-12AR-J4	Circumferential	28%	360°	Weld overlay per Fig. 2.2
2B31-1RC-12AR-K2	Circumferential	19%	360°	Weld overlay per Fig. 2.2
2B31-1RC-12AR-K3	Circumferential	6%	360°	Weld overlay per Fig. 2.2

Table 1.1

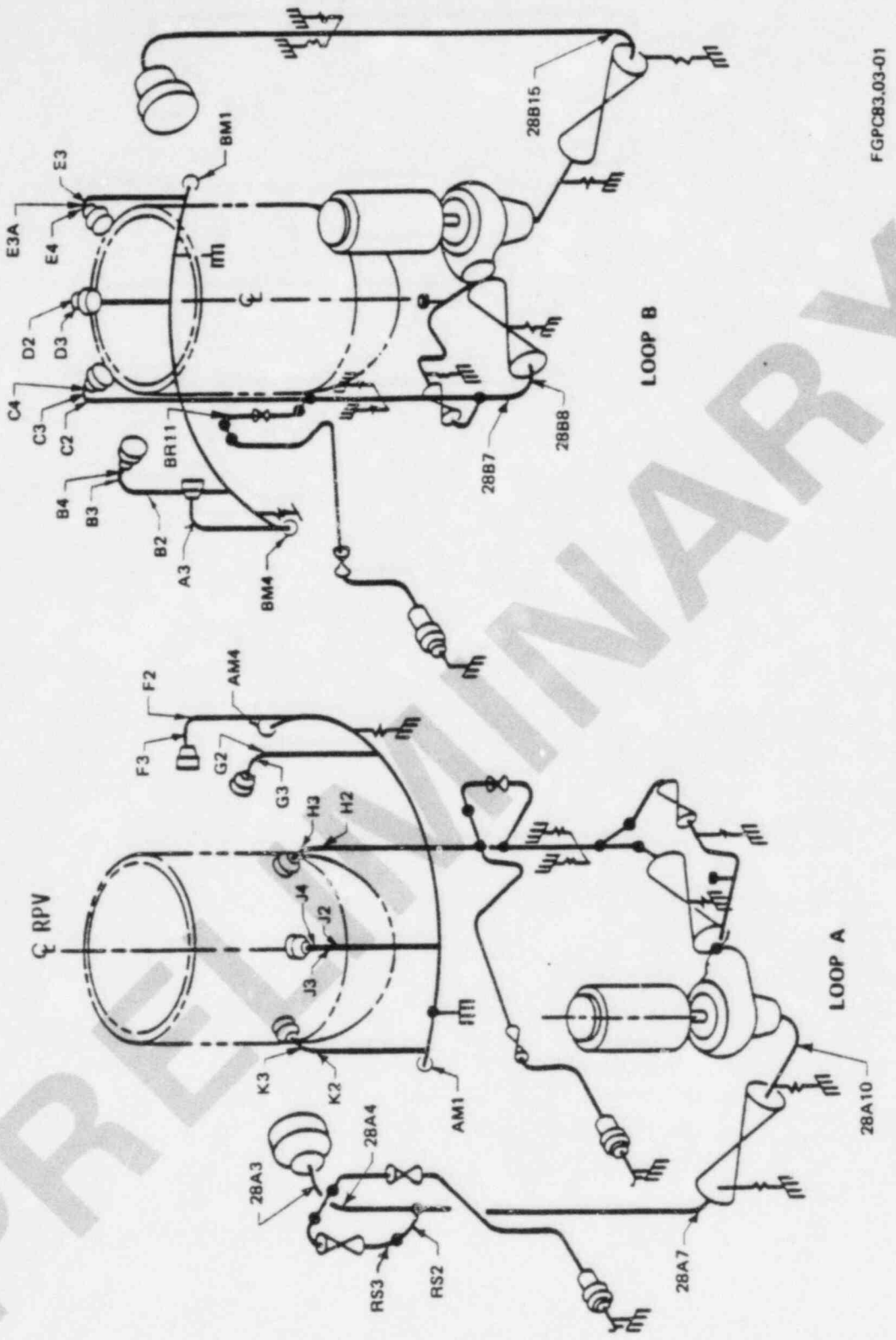

Figure 1.1

CONCEPTUAL DRAWING OF RECIRCULATION SYSTEM

2.0 REPAIR DESCRIPTION

The indications in the existing safe end, 12" elbow, 12" pipe, and three of the four end cap weld heat-affected zones have been repaired by establishing additional "cast-in-place" pipe wall thickness from weld metal deposited 360 degrees around and to either side of the existing weld, as shown in Figures 2.1 through 2.5. The fourth end cap was cut off and replaced with a new equivalent end cap. The weld-deposited band over the cracks will provide wall thickness equal to that required to provide the original design safety margins. In addition, the weld metal deposition will produce a favorable compressive residual stress pattern. The deposited weld metal will be type 308L, which is resistant to propagation of IGSCC cracks.

The non-destructive examination of the weld overlays consisted of:

1) Surface examination of the completed weld overlay by the liquid penetrant examination technique in accordance with ASME Section XI.

2) Volumetric examination of the completed weld overlay by the ultrasonic examination technique in accordance with ASME XI.

3) Volumetric preservice examination of the weld overlay and existing circumferential pipe weld by the ultrasonic examination technique in accordance with ASME Section XI.

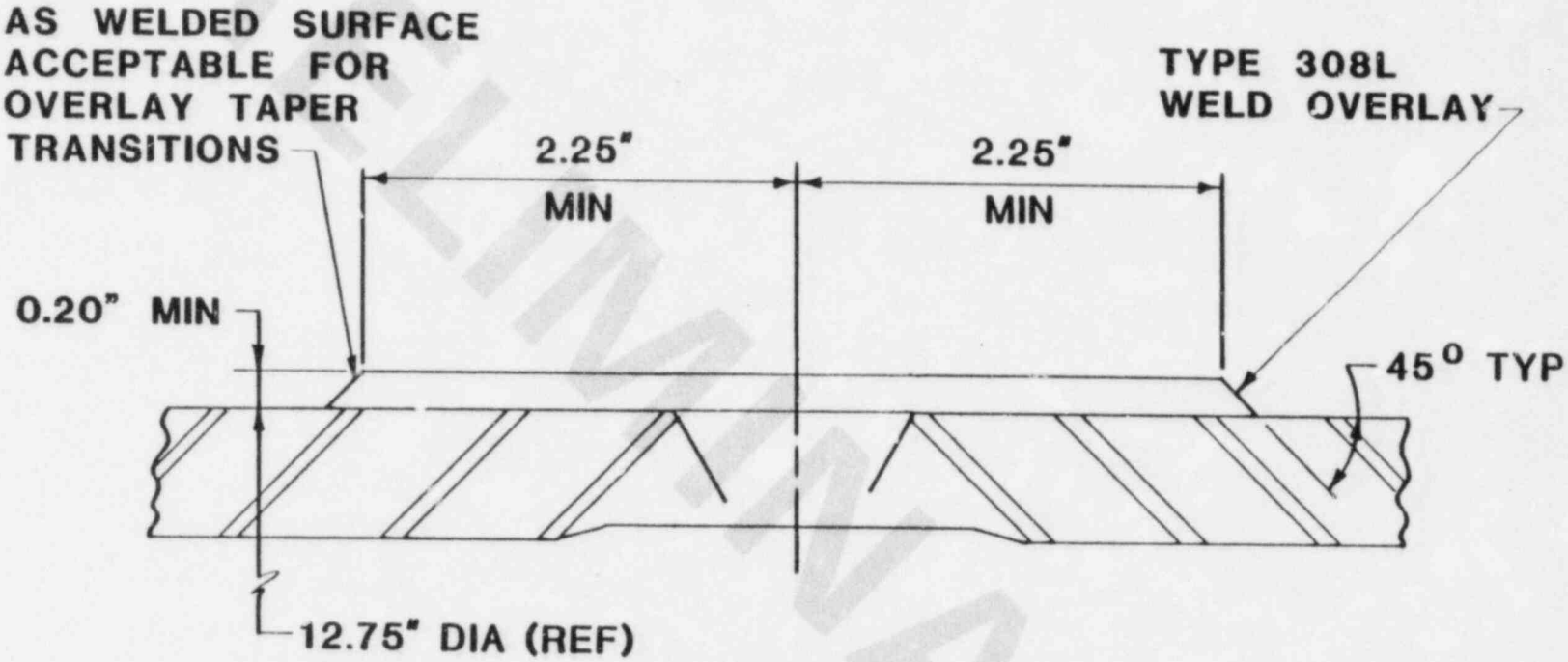

Figure 2.1

STANDARD OVERLAY DESIGN
12" RECIRCULATION WELDS

Patent Applied For

nutech ENGINEERS

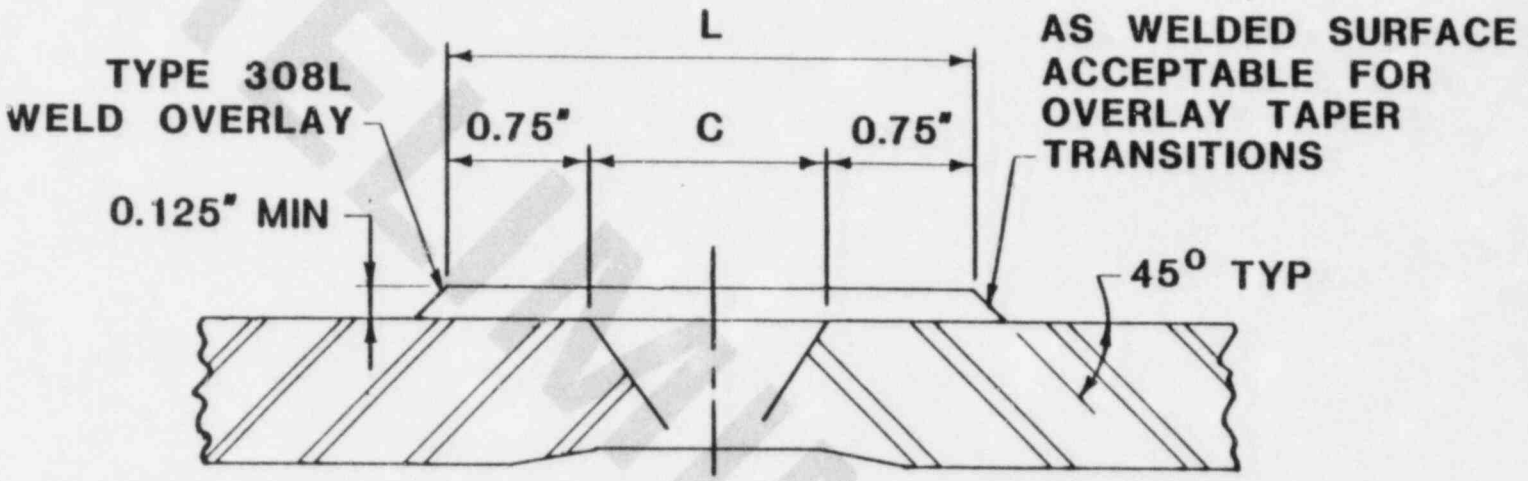

$L_{MINIMUM} = 1.5" + C$

C = WELD CROWN WIDTH

FGPC83.03-04

Figure 2.2

MINI-OVERLAY DESIGN
12" RECIRCULATION WELDS

Patent Applied For

nutech ENGINEERS

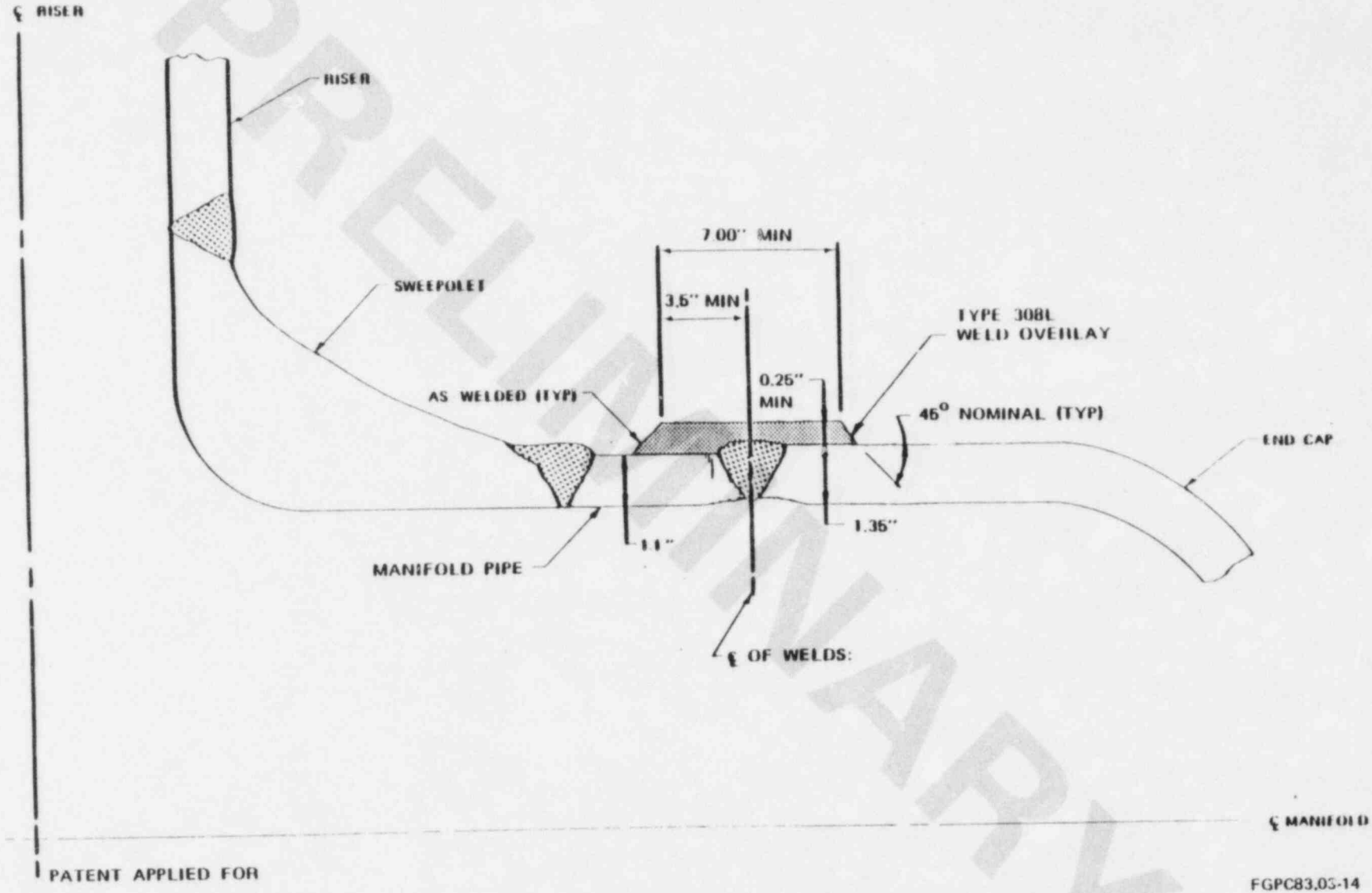

Figure 2.3

CONFIGURATION OF END CAP WELD OVERLAY

3.0 EVALUATION CRITERIA

3.1 Weld Overlay and End Cap Replacement Evaluation

This section describes the criteria that are applied in this report to evaluate the acceptability of the weld overlay repairs and end cap replacement described in Section 2.0. Because of the nature of these repairs, the geometric configuration is not directly covered by Section III of the ASME Boiler and Pressure Vessel Code, which is intended for new construction. However, materials, fabrication procedures, and Quality Assurance requirements are in accordance with applicable sections of this Construction Code, and the intent of the design criteria described below is to demonstrate equivalent margins of safety for strength and fatigue considerations as provided in the ASME Section III Design Rules. In addition, because of the IGSCC conditions that led to the need for repairs, ICSCC resistant materials have been selected for the weld overlay repairs. As a further means of ensuring structural adequacy, criteria are also provided below for fracture mechanics evaluation of the repairs.

3.1.1 Strength Evaluation

Adequacy of the strength of the weld overlay repairs and end cap replacement with respect to applied mechanical loads is demonstrated with the following criteria:

1. An ASME Boiler and Pressure Vessel Code Section III, Class 1 (Reference 1) analysis of the weld overlay repairs was performed.

2. The ultimate load capacity of the weld overlay repairs was calculated with a tearing modulus analysis. The ratio between failure load and applied loads was required to be greater than that required by Reference 1.

3.1.2 Fatigue Evaluation

The stress values obtained from the above strength evaluation were combined with thermal and other secondary stress conditions to demonstrate adequate fatigue resistance for the design life of each repair. The criteria for fatigue evaluation include:

1. The maximum range of primary plus secondary stress was compared to the secondary stress limits of Reference 1.

2. The peak alternating stress intensity, including all primary and secondary stress terms, and a fatigue strength reduction factor of 5.0 to account for the existing crack underneath weld overlays, was evaluated using conventional fatigue analysis techniques. The total fatigue usage factor, defined as the sum of the ratios of applied number of cycles to allowable number of cycles at each stress level, must be less than 1.0 for the design life of each repair. Allowable number of cycles was determined from the stainless steel fatigue curve of Reference 1.

3.1.3 Crack Growth Evaluation

Crack growth due to both fatigue (cyclic stress) and IGSCC (steady state stress) was calculated. The allowable crack depth was established based on net section limit load for each cracked and repaired weld (Reference 2). The design life of each repair was

established as the minimum of either the predicted time for the observed crack to grow to the allowable crack depth or five years.

3.2 Flaw Evaluation

Crack growth due to both fatigue (cyclic stress) and IGSCC (steady state stress) was calculated. The allowable crack depth was established based on the net section collapse load for the cracked welds (Reference 2).

The life of the unrepaired welds with observed flaws was established as the time for the flaw to grow to the allowable depth.

4.0 LOADS

The loads considered in the evaluation of the repaired, replaced and unrepaired welds were mechanical loads, internal pressure, differential thermal expansion loads, and welding residual stresses. The mechanical loads and internal pressures used in the analysis are described in Section 4.1, and an explanation of the thermal transient conditions which cause differential thermal expansion loads is presented in Section 4.2. Welding residual stresses are considered in the crack growth analyses and are discussed in Section 5.1.

4.1 Mechanical and Internal Pressure Loads

The design pressures of 1450 psi pump discharge and 1250 for the pump suction portions of the Recirculation System were obtained from Reference 3. The dead weight and seismic loads applied to each weld were also obtained from Reference 3. The design stress for the RHR System were obtained from Reference 4.

4.2 Thermal Loads

The thermal expansion loads for each weld were obtained from Reference 3 for the Recirculation System and from Reference 4 for the RHR System. Reference 5 defines several types of transients for which the Hatch 1 Recirculation and RHR Systems were designed. It was assumed that the Hatch 1 and Hatch 2 designs transients are similar. These transients were conservatively grouped into three composite transients. The first composite transient is a startup/shutdown transient with a heatup or cool down rate of 100°F per hour. The second composite transient consists of a 50°F step temperature with no change in pressure. The third composite transient is an emergency event with a 416°F step temperature change and a pressure change of 1325 psi. In the five year overlay design life, there are 38 startup/shutdown cycles, 25 small temperature change cycles, and one emergency cycle.

5.0 EVALUATION METHODS AND RESULTS

The evaluation of the welds consist of a code stress analysis per Section III (Reference 1) and a fracture mechanics evaluation per Section XI (Reference 6).

5.1 Weld Residual Stress Calculation and Measurement

5.1.1 Residual Stress Calculation

The residual stresses that exist in the weld heat affected zone after application of the weld overlays were calculated using the methodology of Reference 17 for each repair geometry.

The analysis consists of four steps:

1. Temperature analysis for welding the butt weld.
2. Residual stress analysis for welding.
3. Temperature analysis for welding the overlay.
4. Residual stress analysis for the overlay.

The temperature analysis is based on heat flow from the point source moving in a straight line in an infinite solid. Boundary conditions are imposed by superimposing auxiliary heat sources to give insulated pipe

surfaces. The temperature profiles generated for each weld pass, both in the heating and cooling phases, then serve as input to the finite element residual stress analysis model. The welding parameters assumed for the analysis of the original butt-welds are shown in Table ___ (Reference 18), and are representative of those used in practice. The weld overlay parameters are also shown in Table ___.

The residual stress model is an axisymmetric finite element representation. Material properties are temperature dependent and the stress-strain behavior is elastic-plastic. Elastic unloading is allowed from a yielded element. Deformation and stress profiles are computed at selected steps during welding.

An axisymmetric finite element mesh was generated for each stress analysis. The stress analysis uses temperature dependent material properties and a bilinear stress strain curve. The Prandtl-Reuss equations for plasticity are used. Residual forces are applied at the end of each incremental solution. At the beginning of each heating or cooling phase an iteration on the stiffness matrix is made to take into account the non-proportional loading due to an abrupt change in the load path.

The transient thermal loading from the welding process was imposed on the structural model by applying the temperature distributions from the thermal analysis in several piecewise linear changes.

The axial and circumferential stress profiles along the inner pipe surface for each geometry after welding are shown in Figures ___ through ___. Also shown in Figures ___ and ___ are residual stress data that were obtained by strain gage techniques by Vertossa, et. al. (Reference 18). Comparisons of the calculated and measured data generally show good agreement, with the calculated results being conservative (i.e., more tensile).

Starting with the original butt-weld stress distribution and the weld overlay temperature distributions, the residual stresses for each repair were calculated.

The resulting stress distributions in the heat affected zone are presented in Figures ___ through ___. From Figures ___ and ___, it is seen that the weld overlay produces significant axial compressive stress in the original pipe cross section. This stress profile will stop or considerably slow the growth of cracks.

The overlay places the inside half of the cross section in circumferential compression stress as shown in Figure ___. This should stop all axial crack growth.

A study of the effect of a circumferential crack on the calculated residual stress due to an overlay has been performed. The results are shown in Figure ___.

5.1.2 Residual Stress Measurements

In order to empirically confirm the analytical residual stress calculations described above, Georgia Power Company is conducting a test program to measure the effect which application of a weld overlay has on residual stresses. This test program is described in detail in References 19 and 20.

The test will attempt to monitor temperatures and stresses (via thermocouples and strain gages) at various locations on a 12 inch stainless steel pipe during application of a weld overlay.

The results will be compared with the analytical predictions described in Section 5.1.1.

5.2 Weld Repair and Evaluation

5.2.1 12" Recirculation Inlet Safe End Evaluation

The heat affected zones on the piping side of the weld between four recirculation inlet safe ends and the recirculation piping had indications. Three of the indications had maximum depth of less than 30% of the wall thickness, thus the mini overlay shown in Figure 2.2 was used. The 12BRC-4 weld had an indication with a maximum depth of 32% of the wall thickness; therefore the standard overlay shown in Figure 2.1 was used.

5.2.1.1 Code Stress Analysis

The ASME Code stress analyses of the four repaired safe end welds were performed with ANSYS (Reference 7) finite element models. The models were based on an overlay thickness of 0.20 inch and 0.125 inch (standard and mini), which are smaller than the actual minimum average thicknesses of (___) inch. Figures 5.1 and 5.2 show the models. The stress in the overlaid safe ends due to design pressure and applied moments as described in Sections 4.1 and 4.2 were calculated with the finite element models.

The weld overlay thermal model was taken to be axisymmetrical (Figure 5.3). The exterior boundary was assumed to be insulated. The temperature distribution in the weld overlay subject to the thermal transients defined in Section 4.2 can be readily calculated using Charts 16 and 23 of Reference 8. The maximum through wall temperature difference was determined to be less than 2°F for the normal startup cycle, 40°F for the small temperature cycle and 329°F for the emergency transient.

The maximum thermal stress for use in the fatigue crack growth analysis was calculated as follows: (Reference 1)

$$\sigma = \frac{Ea\Delta T_1}{2(1-\nu)} + \frac{Ea\Delta T_2}{1-\nu}$$

Where:

E = 28.3×10^6 psi (Young's Modulus)

a = $9.11 \times 10^{-6} {}^\circ F^{-1}$
(Coefficient of Thermal Expansion)

ΔT_1 = Equivalent Linear Temperature Difference

ΔT_2 = Peak Temperature Difference

The values of ΔT_1, ΔT_2, and σ are given in Table 5.1 for all three thermal transients.

The results of Code stress analyses of the standard and the limiting mini overlays per Reference 1 are given in Table 5.2. The allowable stress values from Reference 1 are also given. The weld overlay repairs satisfy the Reference 1 requirements.

A conservative fatigue analysis per Reference 1 was performed. In addition to the stress intensification factors required per Reference 1, an additional fatigue strength reduction factor of 5.0 was applied due to the crack. The fatigue usage factor was then calculated assuming 38 startups, 25 small temperature change cycles and one emergency cycle every five years. The results are summarized in Table 5.2.

5.2.1.2 Fracture Mechanics Evaluation

Three types of fracture mechanics evaluations were performed. The allowable crack depth was calculated based on Reference 2. Crack growth due to both fatigue and IGSCC was calculated using the NUTECH computer program NUTCRAK (Reference 9) with material constants and methodology from References 10 and 11. Finally, the

ultimate margin to failure for a crack assumed to propagate all the way through the original pipe material to the weld overlay was calculated per References 12 and 13.

The allowable crack depth for a 360° circumferential crack in the overlaid welds was determined based on Reference 2. The allowable crack depth is ___ percent of the overlaid (___) weld thickness. Thus, the allowable crack depth for a 360° circumferential crack is (___) inch.

The existing cracks could grow due to both fatigue and stress corrosion. Fatigue crack growth due to the three types of thermal transients defined in Section 4.2 was calculated using the material properties from Reference 10. The fatigue cycles considered are shown in Figure 5.4. The fatigue crack growth for 5 years was calculated to be less than 0.01 inch.

IGSCC crack growth was calculated using the overlay residual stress distribution shown in Figure ___. The steady state loads of pressure, dead weight and thermal expansion were also applied. The results are shown in Figure ___.

The weld overlay is not susceptible to IGSCC. Thus the maximum depth after five years of a 360° circumferential crack is approximately ___ inch. Based on Section 5.1.2.1 a circumferential crack of that size is acceptable.

Thus, the overlay design is acceptable for five years.

5.2.1.3 Tearing Modulus

The largest size to which the existing crack could reasonably be expected to grow was postulated to be a 360° circumferential crack of depth equal to that given in Section 5.1.2.2. A tearing modulus evaluation was then performed for this postulated crack. The applied loads were pressure, weight, seismic, and thermal expansion.

The evaluation was performed using the methodology of Reference 12 with material properties from Reference 13.

The postulated flaw and the results are shown in Figure 5.6. The upper dotted line represents the inherent material resistance to unstable fracture in terms of J-integral and Tearing Modulus, T. The line originating at the origin represents the applied

loading. Increasing load results in applied J-T combinations moving up this line, and unstable fracture is predicted at the intersection of this applied loading line with the material resistance line.

Figure 5.6 shows that the predicted failure load is in excess of ___ times the normal applied loads. Thus, there is a safety factor on normal loads (including OBE seismic) of at least ___, which is well in excess of the safety factor inherent in the ASME Code, even in the presence of this worst case assumed crack.

5.2.2 12" Elbow and Pipe-to-Pipe Evaluation

The heat affected zone of the weld between eighteen recirculation inlet elbow and risers have UT indications. In addition, one 12" pipe to pipe weld has indications. To ensure a conservative overlay design, it was assumed that a 360° circumferential crack exists in the welds, with maximum depths as shown in Table 1.1. Eighteen of the nineteen welds were repaired with the mini design (Figure 2.2) and one weld, 12BR-C3, was repaired with the standard design (Figure 2.1). The pipe to pipe weld was repaired with the mini design.

5.2.2.1 Code Stress Analysis

Finite element models of the repaired regions were developed using the ANSYS (Reference 7) computer program. The models were based on an overlay thickness of 0.20 inch for the standard overlay (Figure 2.1) and 0.125 inch for the mini-overlay (Figure 2.2). Figures 5.7 and 5.8 show the models. This figure also shows the material that was removed to represent the crack.

The stress in the overlaid elbow due to design pressure and applied moments as described in Sections 4.1 and 4.2 was calculated with the finite element models. The thermal analysis was performed in the same manner as for the safe end (Section 5.2.1), with appropriate dimensional changes.

The results of a code stress analysis per Reference 1 are given in Table 5.3. The allowable stress values from Reference 1 are also given. The weld overlay repairs satisfy the Reference 1 requirements.

A conservative fatigue analysis per Reference 1 was performed. A fatigue strength reduction factor of 5.0 was applied due to the crack. The fatigue usage factor

was then calculated assuming 38 startups, 25 small temperature change cycles and one emergency cycle every 5 years. The results are summarized in Table 5.3.

5.2.2.2 Fracture Mechanics Evaluation

Three types of fracture mechanics evaluations were performed. The allowable crack depth was calculated based on Reference 2. Crack growth due to both fatigue and IGSCC was calculated using the NUTECH computer program NUTCRAK (Reference 9) with material constants and methodology from References 10 and 11. Finally, the ultimate margin to failure for the assumed crack was calculated per References 12 and 13.

The design minimum overlay thicknesses of 0.125 or 0.20 inch were established (References 2) based on a 360° circumferential crack. The minimum average as-built overlay thicknesses are ____ inch. The allowable crack depth for a 360° crack with a standard overlay thickness of ____ inch is ____ inch. The allowable crack depth for a 360° crack with a mini overlay thickness of ___ inch is ___ inch.

IGSCC crack growth was calculated using the overlay residual stress pattern shown in Figure ___. The steady state loads of pressure, dead weight and thermal expansion were also applied. The results are shown in Figure ___. The fatigue crack growth due to five years of the cycles shown in Figure 5.4 is less than 0.01 inch. Maximum depth after five years is predicted to be ___ which is less than the allowable depth of ___.

5.2.2.3 Tearing Modulus

A tearing modulus evaluation was performed for the assumed 360° crack. The normal operating loads of OBE seismic, pressure, weight and thermal expansion were applied.

The evaluation was performed using the methodology of Reference 12 with material properties from Reference 13. The postulated flaw and the results are shown in Figure 5.9. The upper dotted line represents the inherent material resistance to unstable fracture in terms of J-integral and Tearing Modulus, T. The line originating at the origin represents the applied loading. Increasing load results in applied J-T

combinations moving up this line, and unstable fracture is predicted at the intersection of this applied loading line with the material resistance line.

Figure 5.9 shows that the predicted failure loads is in excess of ___ times the normal operating loads. Thus, there is a safety factor on normal operating loads, including OBE seismic, of at least ___, which is in excess of the safety factor inherent in the ASME Code, even in the presence of this worst case assumed crack.

5.2.3 22" End Cap Repair Evaluation

The heat affected zones of four of the welds between the 22" pipe and the end cap have several circumferential UT indications. The largest of the indications was estimated to have a depth of approximately 42% percent of the wall thickness.

5.2.3.1 Code Stress Analysis

A finite element model of the repaired end caps was prepared using ANSYS as above. This model is shown in Figure 5.10. The stress in the end cap due to design pressure as described in Section 4.1 was calculated with the finite element model. The thermal analysis was

performed in the same manner as for the safe end (Section 5.2.1), with appropriate dimensional changes.

The results of a Code stress analysis per Reference 1 are given in Table 5.4. The allowable stress values from Reference 1 are also given. The repaired end cap configuration satisfies the Reference 1 requirements.

A conservative fatigue analysis per Reference 1 was performed. A fatigue strength reduction factor of 5.0 was applied due to the assumed crack. The fatigue usage factor was then calculated assuming 38 startups, 25 small temperature change cycles and one emergency cycle every five years. The results are summarized in Table 5.4.

5.2.3.2 Fracture Mechanics Evaluation

Three types of fracture mechanics evaluations were performed. The allowable crack depth was calculated based on Reference 2. Crack growth due to both fatigue and IGSCC was calculated using the NUTECH computer program NUTCRAK (Reference 9) with material constants and methodology from References 10 and 11. Finally, the ultimate margin to failure for the assumed crack was calculated per References 12 and 13.

The existing cracks could grow due to both fatigue and stress corrosion. Fatigue growth due to the three types of thermal transients defined in Section 4.2 was calculated using the material properties from Reference 10. The fatigue crack growth for five years of the cycles shown in Figure 5.4 was calculated to be less than 0.01 inch.

IGSCC crack growth was calculated using the upper bound crack growth law shown in Figure 5.5. The residual stress was based on both the original butt weld residual stress and that due to the overlay as shown in Figure ____. The crack growth analysis was performed with the NUTECH computer program NUTCRAK (Reference 9). Crack growth as a function of time was determined for a circumferential crack of size described in Section 5.3. Maximum crack depth after five years is predicted to be ____ inch which is well below the allowable of ___ inches.

5.2.3.3 Tearing Modulus

A tearing modulus evaluation was performed for a crack of depth equal to ____. The normal operating loads of OBE seismic, pressure, weight and thermal expansion were

applied. The evaluation was performed using the methodology of Reference 12 with material properties from Reference 13.

The postulated flaw and the results are shown in Figure ____. The upper dotted line represents the inherent material resistance to unstable fracture in terms of J-integral and Tearing Modulus, T. The line originating at the origin represents the applied loading. Increasing load results in applied J-T combinations moving up this line, and unstable fracture is predicted at the intersection of this applied loading line with the material resistance line.

Figure ____ shows that the predicted failure load is in excess of ___ times the normal operating loads. Thus, there is a safety factor on normal operating loads, including OBE seismic, of at least ___, which is in excess of the safety factor inherent in the ASME Code, even in the presence of this worst case assumed crack.

5.2.4 End Cap Replacement Evaluation

(LATER)

5.3 Evaluation of Unrepaired Flaws

UT examination of the large diameter Recirculation and RHR. System at Plant Hatch Unit 2 has revealed twelve welds which have reportable indications. Nine of the welds with reportable indications are in the 28 inch diameter Recirculation Piping, one is in the 24 inch diameter RHR Piping, and two are in the 20 inch diameter RHR Piping. The location of each of these defects is shown in Figure 1.1. All of these indications are circumferentially oriented.

IGSCC crack growth in large diameter piping is different than IGSCC crack growth in small diameter piping due to a significant difference in the original butt weld residual axial stress. In large diameter piping there is a significant portion of the pipe thickness near the inside surface which is in compression as shown in Figure 5.12. In small diameter piping typically the inside one-half of the pipe thickness experiences axial residual tensile stress. Thus, shallow circumferential flaws in large diameter piping will generally grow significantly slower than similar flaws in small diameter piping. The following Sections provide the results of crack growth analyses of the flaws in large diameter Recirculation and RHR Piping.

5.3.1 28 Inch Recirculation Piping

Nine welds in the 28 inch diameter Recirculation Piping have reportable UT indications. All the welds with reportable UT indications are pipe-to-elbow welds. All UT indications are circumferentially oriented. The flaws are tabulated in Table 1.1 and their location is shown in Figure 1.1.

Weld number 28B-15 has the highest value of primary stress and contains the largest UT indication. Thus, the allowable crack depth for weld 28B-15 will be bounding for any of the crack indication locations in the 28" Recirculation Piping. The allowable crack depth for weld 28B-15 was determined based on Reference 2 to be 63% of the pipe wall thickness.

The predicted growth of each of the existing UT indications requires several inputs:

1) Steady state applied stress
2) Weld residual stress
3) Flaw characterization
4) Crack growth model
5) Crack growth law

The approach was to use conservative input for applied stress, residual stress, crack growth model and crack growth law. Thus, the result of the analysis is a very conservative prediction of crack size versus time.

The steady state loads at each crack location due to operating pressure, dead weight and thermal expansion were obtained from Reference 3. The steady state stresses were then calculated based on design minimum weld preparation wall thickness ("C" dimension) at each specific location.

The weld residual stress was obtained from a set of NUTECH standard residual stress curves (Reference 14). The residual axial stress curve for large bore piping from Reference 14 is shown in Figure 5.12. This residual stress curve was used for each crack growth analysis.

The flaw sizes are tabulated in Table 1.1. It was conservatively assumed that each crack was full depth for the entire crack length.

The crack growth law is the upper bound law from Reference 10 and is given below: (Figure 5.5)

$$\frac{da}{dT} = 4.116 \times 10^{-12} K^{4.615}$$

da = Differential crack size

dT = Differential time

K = Applied stress intensity factor

The crack growth model is an edge cracked plate. This model is very conservative when applied to an inside diameter crack cylinder because the cracked-plate model introduces extra bending stresses which are tensile at the crack location. The magnitude of this conservatism will be discussed below.

The predicted crack growth of each of the nine cracked welds was calculated with the NUTECH Computer Program NUTCRAK (Reference 9). The limiting crack is in weld 28B-15. Figure 5.13 is a plot of the stress intensity factor for both applied and residual stresses versus crack depth for weld 28B-15. Figure 5.14 is a plot of the predicted crack depth as a function of time for weld 28B-15. Examination of Figure 5.14 will show that the UT indication will not grow to the allowable size for at least 26 months.

Another way of expressing the same margin is to determine the crack size-that would grow to the allowable crack size in the next 18 month fuel cycle. From Figure 5.14 for weld 28B-15, a crack size of 29% would grow to the allowable of 63% in 18 months. Thus, the currently allowable crack size is 29%, which is 1.25 times the largest measured crack size. The predicted crack growth for all nine UT indications are tabulated in Table 5.5.

The results tabulated in Table 5.5 are very conservative due to the conservative method used in the crack growth calculation. One of the largest conservatisms is the use of an edge cracked plate model instead of an inside diameter crack cylinder model. Repeating the above crack growth analysis for weld 28B-15 with an inside diameter cracked cylinder model results in a time of approximately 320 months before the crack would grow to the allowable size or alternately a currently allowable size which is more than 2.5 times the measured crack size.

5.3.2 24 Inch RHR Piping

One weld (24BR-11) in the 24 inch diameter RHR Piping nas reportable UT indications. The weld with reportable UT indications is a pipe-to-elbow weld. The UT indications are circumferentially oriented. The flaws are tabulated in Table 1.1 and their location is shown in Figure 1.1.

The allowable crack depth for weld 24BR-11 was determined based on Reference 2 to be ____ of the pipe wall thickness.

The predicted crack growth of weld 24BR-14 was calculated using the method described in Section 5.3.1. The results are tabulated in Table 5.5.

5.3.3 20 Inch RHR Piping

Two welds in the 20 inch diameter RHR Piping have reportable UT indications. Both of the welds with reportable UT indications are pipe-to-elbow welds. All UT indications are circumferentially oriented. The flaws are tabulated in Table 1.1 and their location is shown in Figure 1.1.

Weld number 20RS-3 has the highest value of primary stress and contains the largest UT indication. Thus, the allowable crack depth for weld 20RS-3 will be bounding for both of the crack indication locations in the 20 inch RHR Piping. The allowable crack depth for weld 20RS-3 was determined based on Reference 2 to be ____ of the pipe wall thickness.

The predicted crack growth of both of the cracks were calculated using the method described in Section 5.3.1. The results are tabulated in Table 5.5.

5.4 Effect on Recirculation and RHR Systems

Installation of the weld overlay repairs caused a small amount of radial and axial shrinkage underneath the overlay. Based on measurements of the weld overlays, the maximum axial shrinkage was ____ inch.

The effects of the radial shrinkage are limited to the region adjacent to and underneath the overlay. Based on Reference 15, the stresses due to the radial shrinkage are less than yield stress at distances greater than 4 inches from the ends of the overlay. Weld residual stresses are steady state secondary stresses and thus are not limited by the ASME Code (Reference 1).

The effect of the axial weld shrinkage on the Recirculation and RHR Systems was evaluated with the NUTECH computer program PISTAR (Reference 16) and the piping model shown in Figure 5.15.

The measured axial shrinkage of all weld overlays were imposed as boundary conditions on this model. Since the ASME Code does not limit weld residual stress, all stress indices were set equal to 1.0.

The maximum calculated stress was less than _____. The location of this stress is shown on Figure 5.12. Steady state secondary stresses of _____ are judged to have no deleterious effect on the Recirculation or RHR Systems.

PARAMETER	NORMAL STARTUP CYCLE (CYCLE 1)	SMALL TEMPERATURE CHANGE CYCLE (CYCLE 2)	EMERGENCY CYCLE (CYCLE 3)
EQUIVALENT LINEAR TEMPERATURE ΔT_1			
PEAK TEMPERATURE ΔT_2			
THROUGH WALL THERMAL STRESS σ			

FGPC83.03-09

Table 5.1
THERMAL STRESS RESULTS

nutech ENGINEERS

CATEGORY	EQUATION NUMBER	ACTUAL STRESS OR THICKNESS	SECTION III NB ALLOWABLE
S	N/A	N/A	S_m = 16,800 PSI
PRIMARY	(9)		25,200 PSI
PRIMARY + SECONDARY	(10)		50,400 PSI
PEAK CYCLE 1 CYCLE 2 CYCLE 3	(11)		N/A
USAGE FACTOR (5 YR)	N/A		1.0

* THE FACTOR OF 5 IS THE CONSERVATIVELY ASSUMED FATIGUE STRENGTH REDUCTION FACTOR.

FGPC83.03-10

Table 5.2

SAFE END CODE STRESS RESULTS

CATEGORY	EQUATION NUMBER	ACTUAL STRESS OR THICKNESS	SECTION III NB ALLOWABLE
S	N/A	N/A	S_m = 14,400**PSI
PRIMARY	(9)		21,600 PSI
PRIMARY + SECONDARY	(10)		43,200 PSI
PEAK CYCLE 1 CYCLE 2 CYCLE 3	(11)		N/A
USAGE FACTOR (5 YR)	N/A		1.0

* THE FACTOR OF 5 IS THE CONSERVATIVELY ASSUMED FATIGUE STRENGTH REDUCTION FACTOR.

** LIMITING LOCATION IS IN THE 308L WELD OVERLAY.

FGPC83.03-11

Table 5.3

12" ELBOW CODE STRESS RESULTS

CATEGORY	EQUATION NUMBER	ACTUAL STRESS OR THICKNESS	SECTION III NB ALLOWABLE
S	N/A	N/A	S_m = 14,400**PSI
PRIMARY	(9)		21,600 PSI
PRIMARY + SECONDARY	(10)		43,200 PSI
PEAK CYCLE 1 CYCLE 2 CYCLE 3	(11)		N/A
USAGE FACTOR (5 YR)	N/A		1.0

* THE FACTOR OF 5 IS THE CONSERVATIVELY ASSUMED FATIGUE STRENGTH REDUCTION FACTOR.

** LIMITING LOCATION IS IN THE 308L WELD OVERLAY.

FGPC83.03-11

5.4

Table ~~5.3~~

~~12" ELBOW~~ CODE STRESS RESULTS

22" END CAP

nutech ENGINEERS

Weld Identification Number	Flaw Depth		Margin	Number of Months Required to Grow to Allowable Depth
	Current	Allowable	Allowable Current Flaw Depth	
2B31-1RC-28A-3	12%	63%	36%	80
2B31-1RC-28A-4	17%	63%	34%	53
2B31-1RC-28A-7	8%	63%	37%	110
2B31-1RC-28A-10	10%	63%		
2B31-1RC-28B-3	15%	63%		
2B31-1RC-28B-7	18%	63%	37%	59
2B31-1RC-28B-8	7%	63%	37%	118
2B31-1RC-28B-10	20%	63%	40%	69
2B31-1RC-28B-15	23%	63%	29%	26
2E11-1RHR-20RS-2	13%			
2E11-1RHR-20RS-3	14%			
2E11-1RHR-24BR-11	18%			

Table 5.5

Crack Growth of Unrepaired Flaws

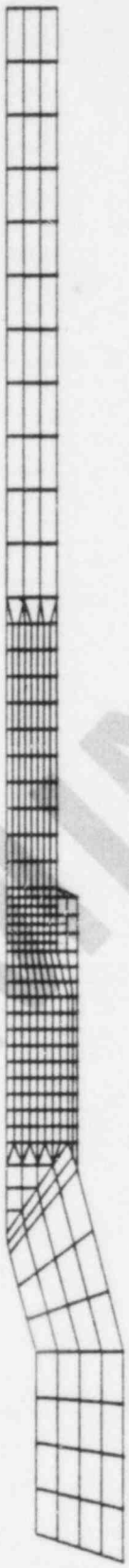

Figure 5.1
SAFE END FINITE ELEMENT MODEL

FGPC83.03-05

nutech ENGINEERS

FIGURE 5.2

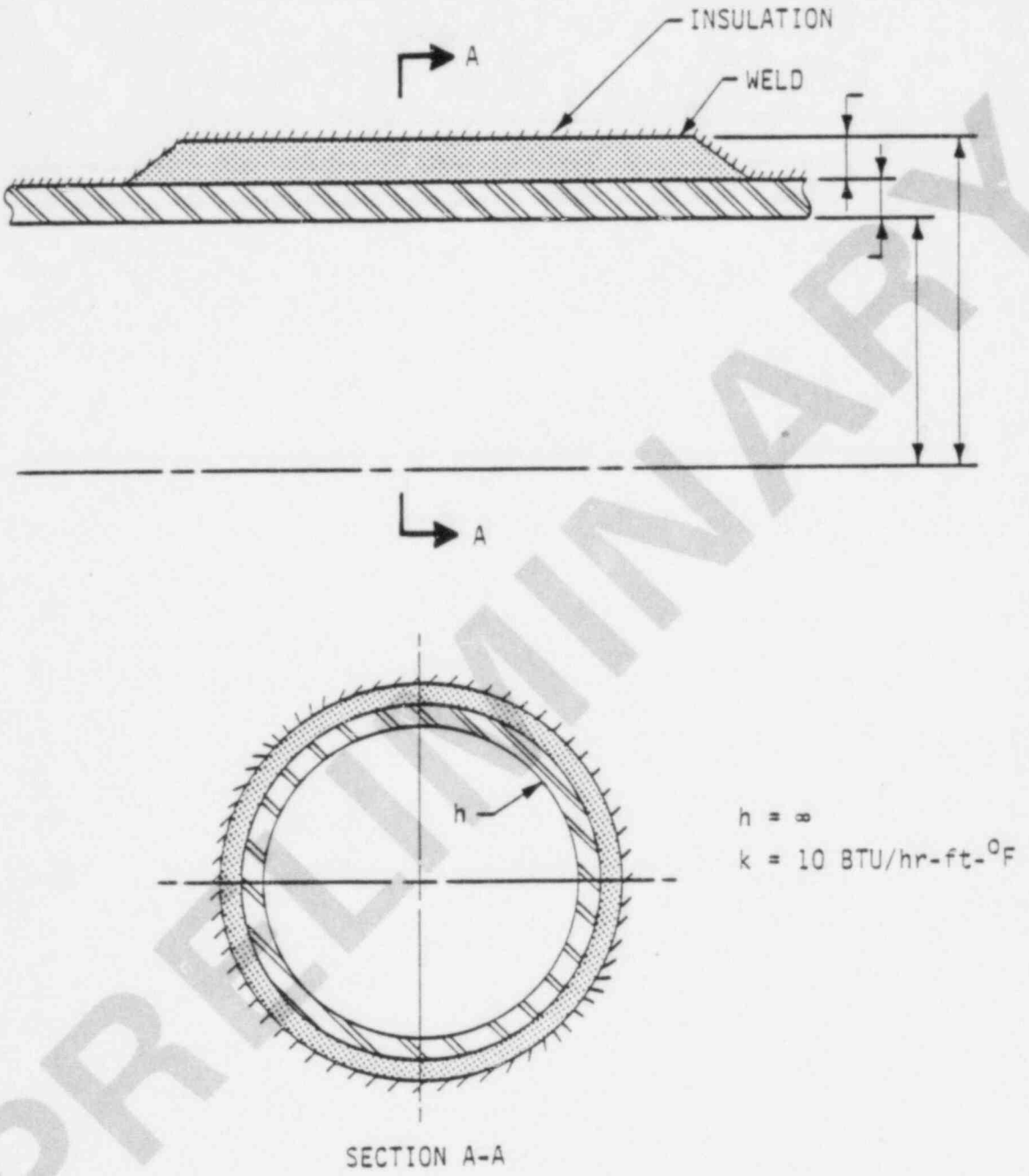

Figure 5.3

WELD OVERLAY THERMAL MODEL

FGPC83.03-0

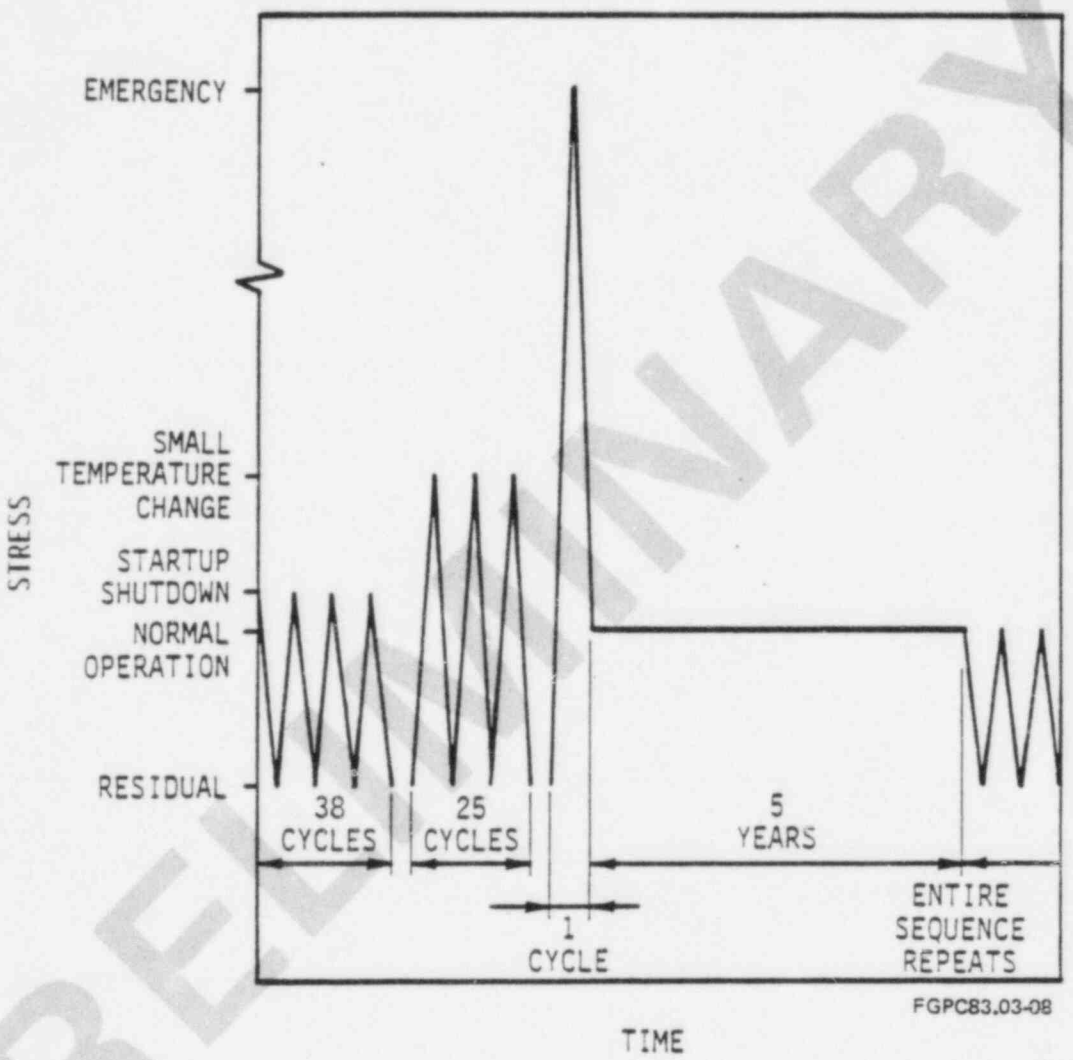

Figure 5.4

THERMAL TRANSIENTS

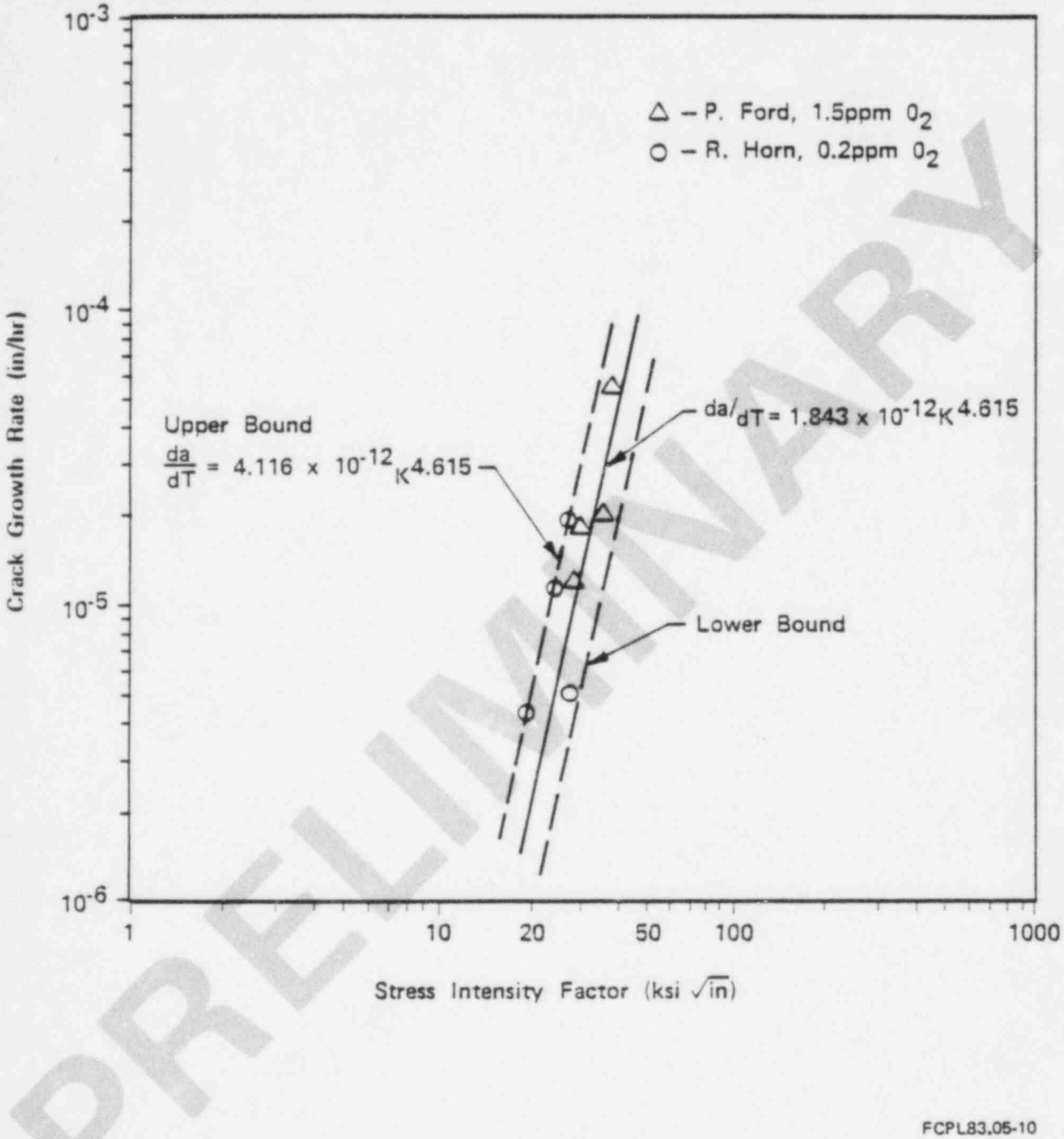

Figure 5.5
TYPICAL IGSCC CRACK GROWTH DATA
(WELD SENSITIZED 304SS IN BWR ENVIRONMENT)

nutech ENGINEERS

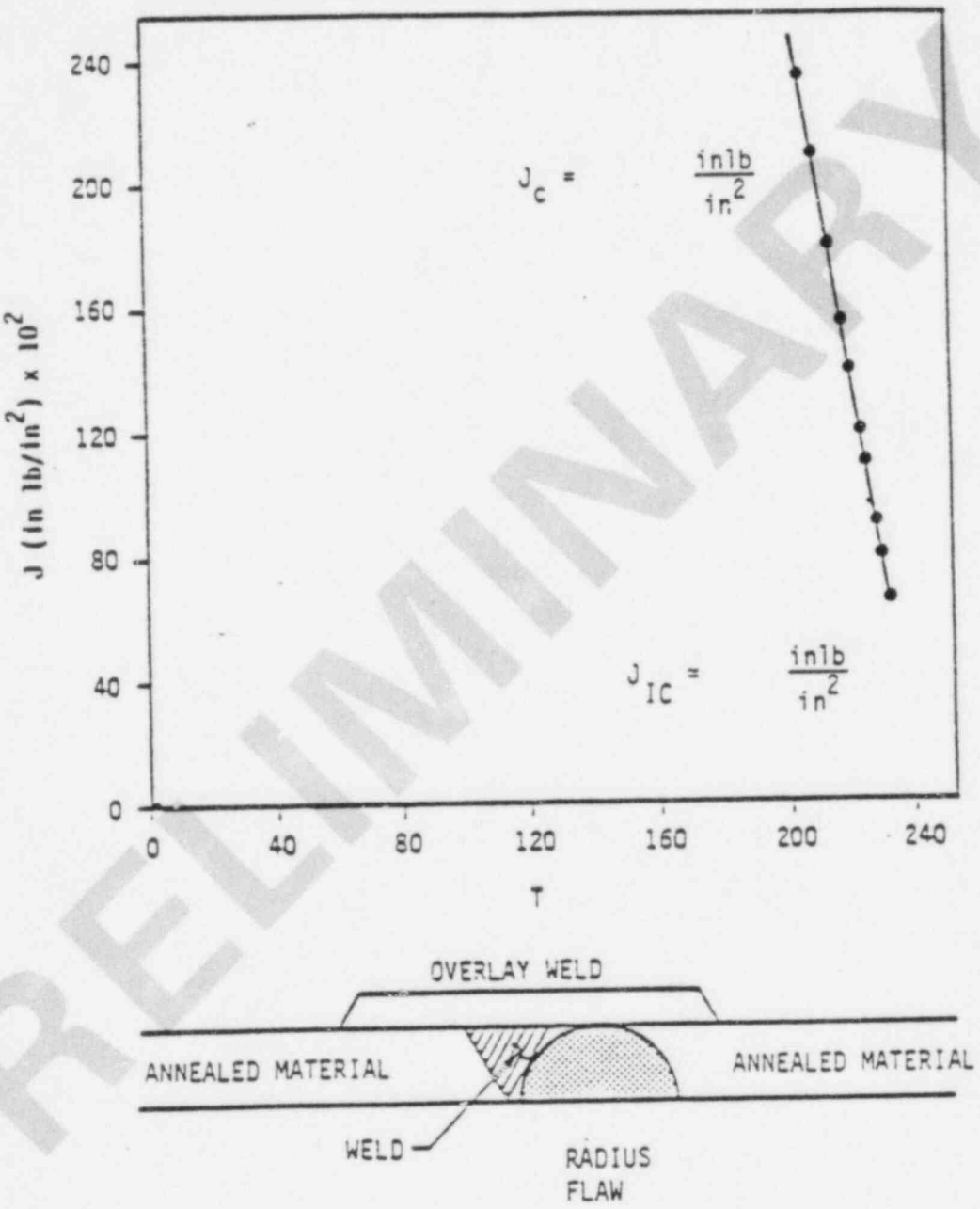

Figure 5.6

SAFE END TEARING MODULUS

FIGURE 5.7

FIGURE 5.8

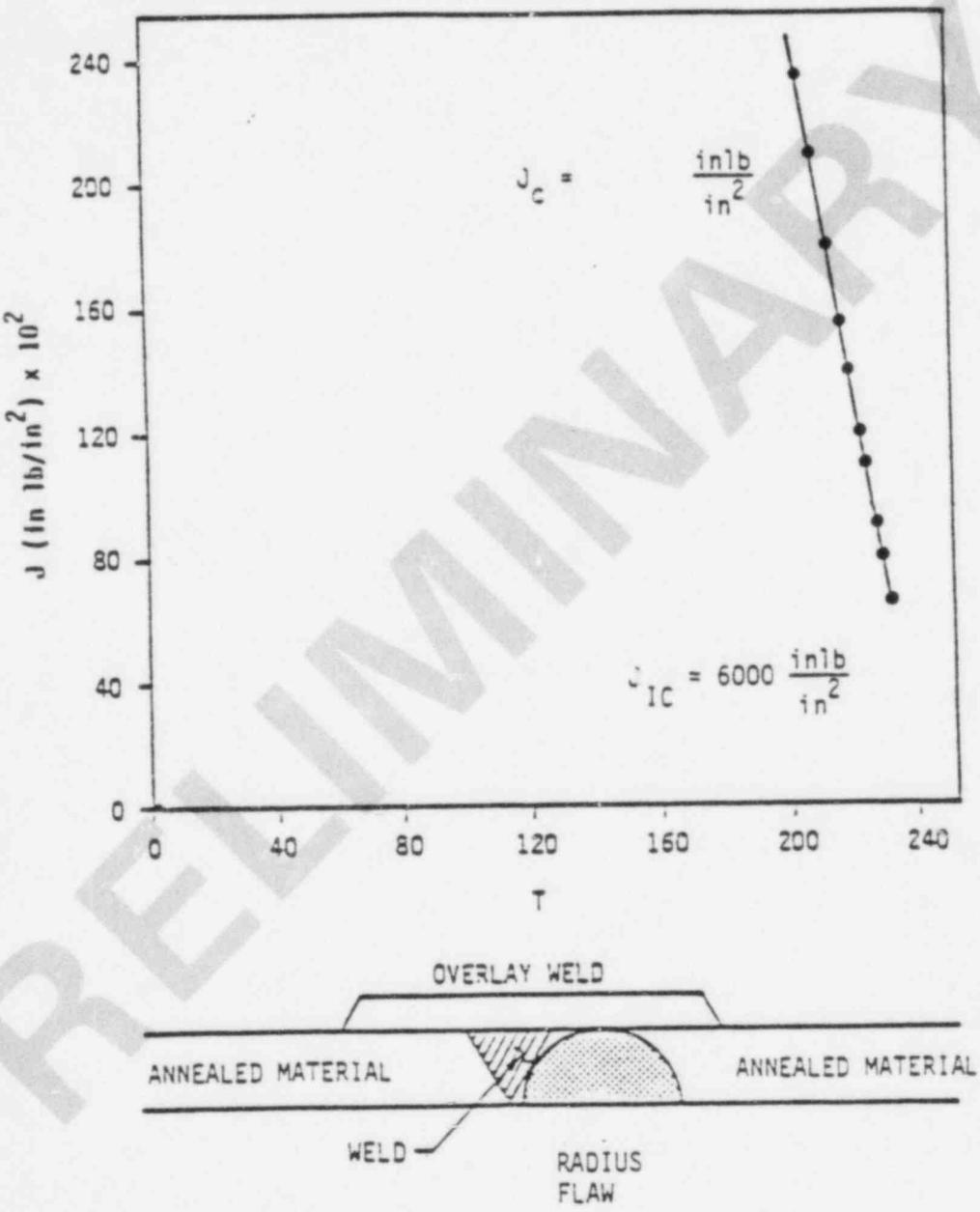

Figure 5.9

12" ELBOW TEARING MODULUS

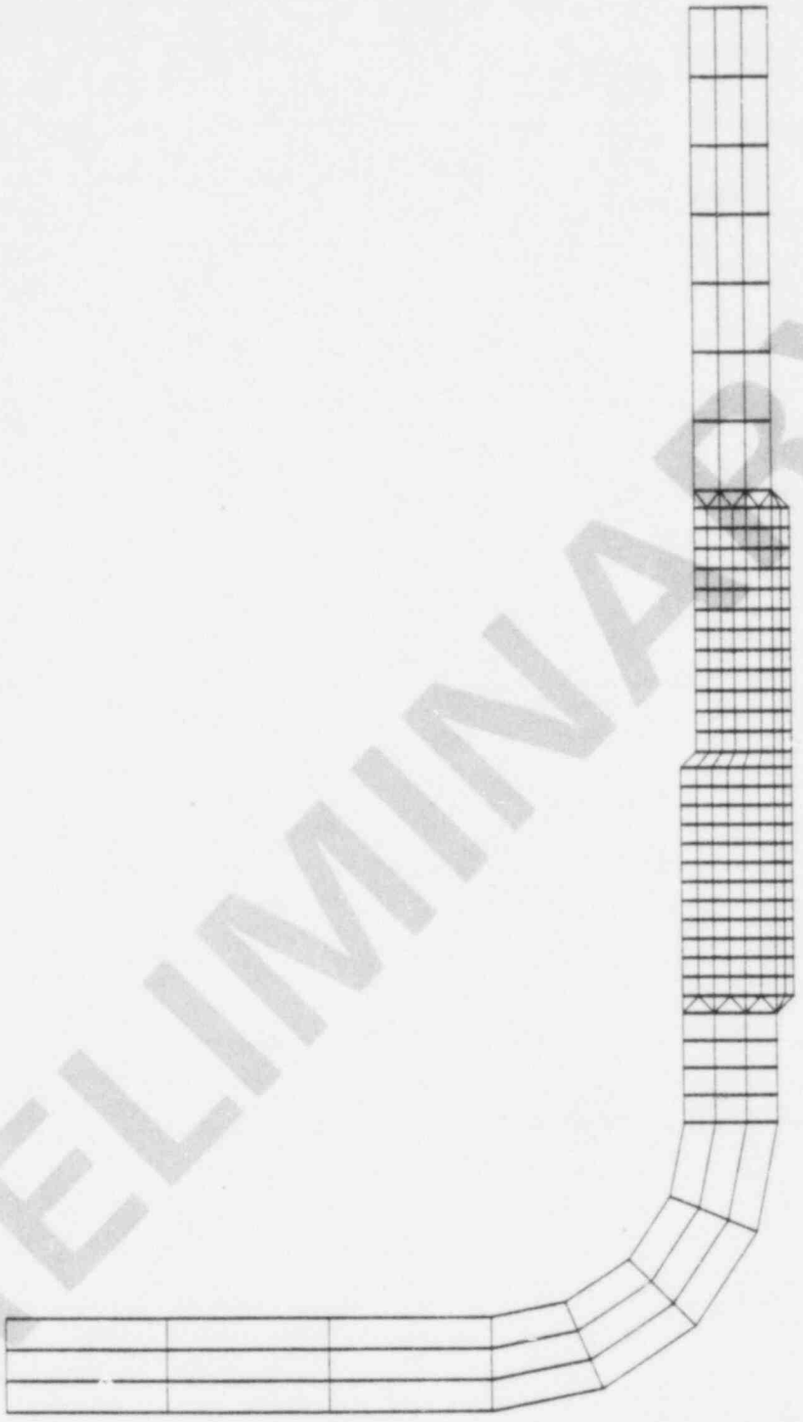

Figure 5.10

END CAP FINITE ELEMENT MODEL

FGPC83.03-07

nutech ENGINEERS

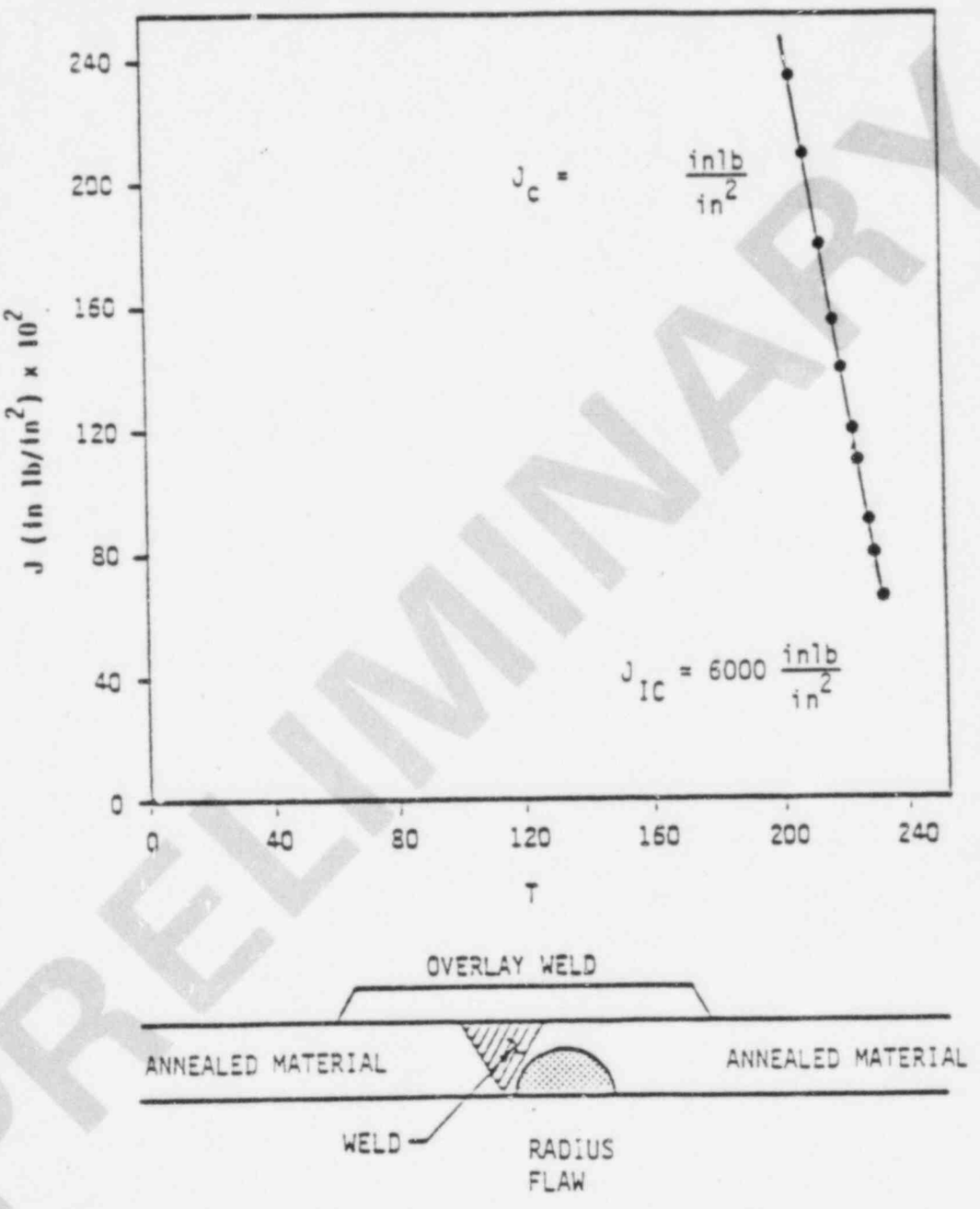

FIGURE 5.11

END CAP TEARING MODULUS

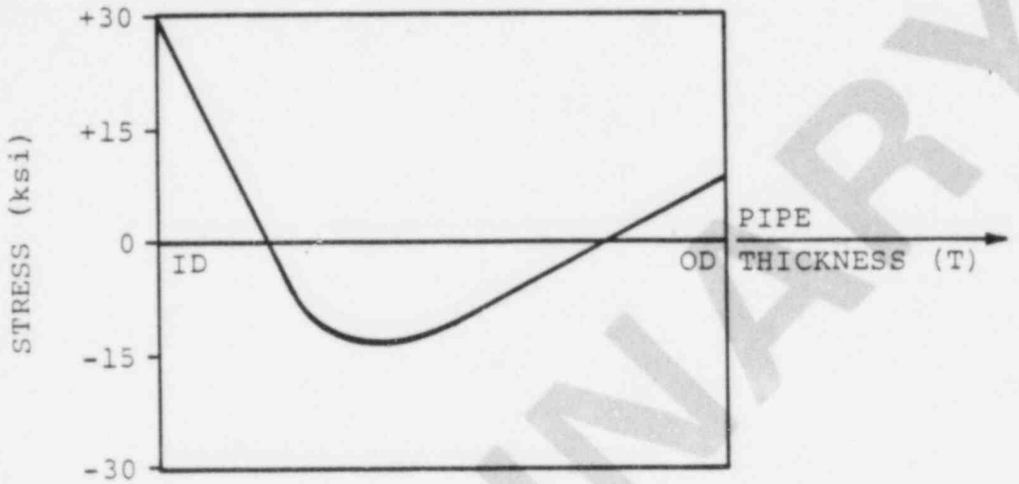

T%	STRESS (ksi)
0	+30.0
19	0.0
25	- 9.9
39	-14.2
50	-12.0
81	0.0
100	+ 8.1

FGPC83.02

FIGURE 5.12

AXIAL RESIDUAL STRESS

PIPE DIAMETER OF 20" TO 28"

nutech ENGINEERS

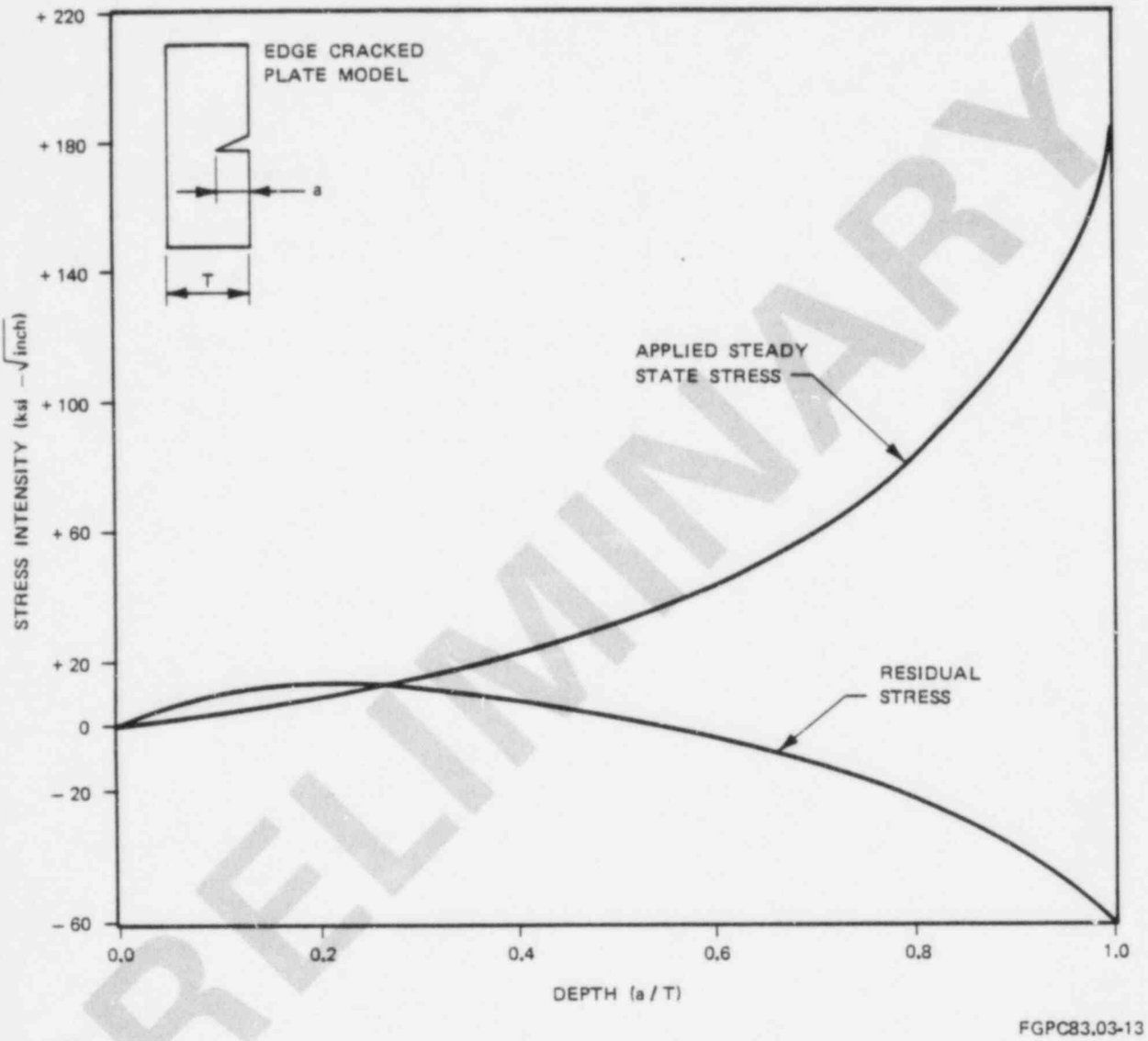

Figure 5.13

STRESS INTENSITY FACTOR FOR WELD 28B – 15

AFQAKMC 83/05/20 08.23.35

IGSCC GROWTH ANALYSIS (CIR. CRACK)
P-EL WELD (ISI WELD ID : B15) (OD=28. IN, T=1.384 IN) (ELBOW SIDE)

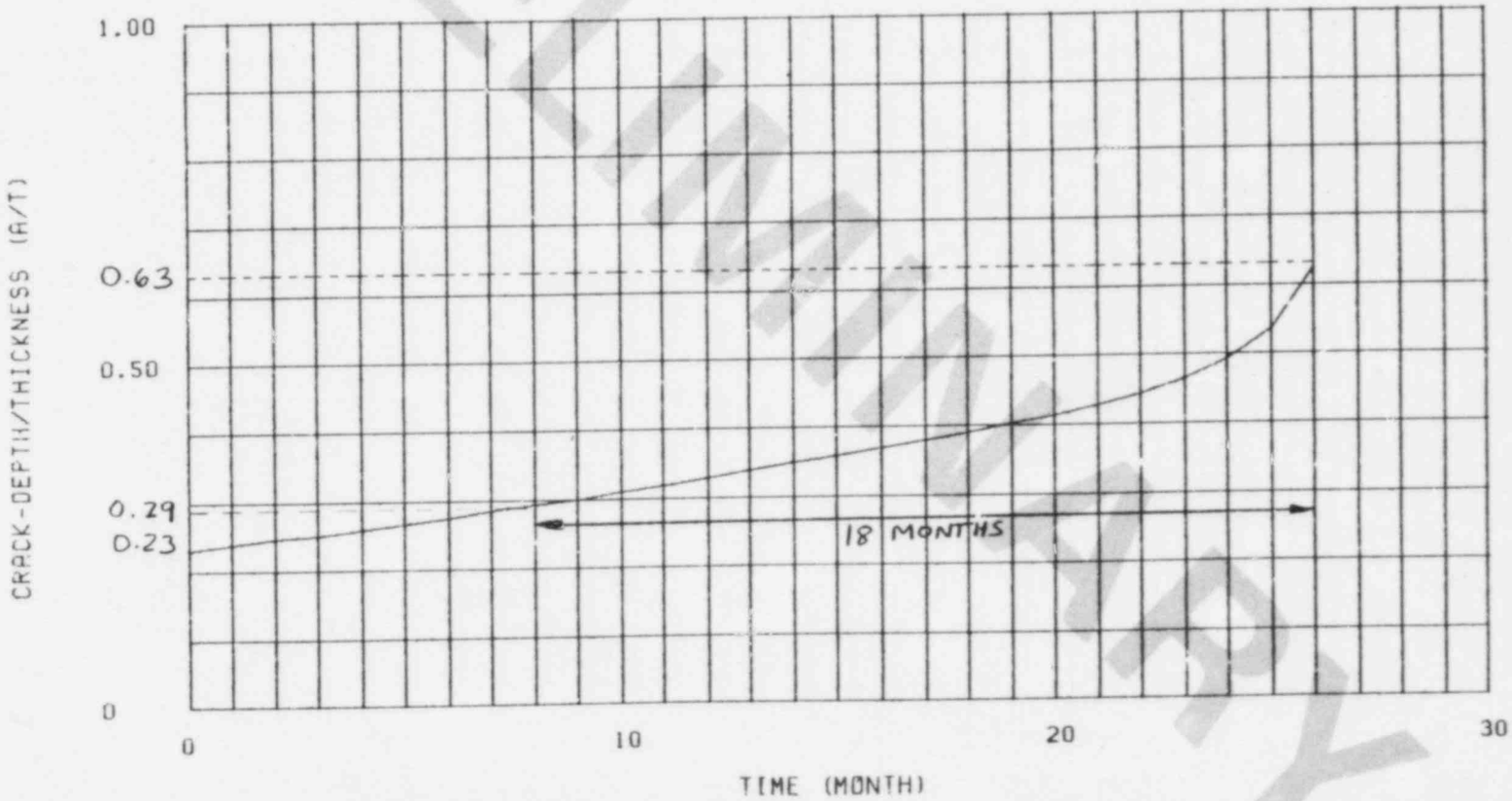

FIGURE 5.14. WORST CASE CRACK GROWTH FOR WELD 28B15

——— NUTCRAK FUN1 (REF. AFQAKJG)
- - - - - - - ALLOWABLE A/T AT THE END OF FUEL CYCLE

nutech ENGINEERS

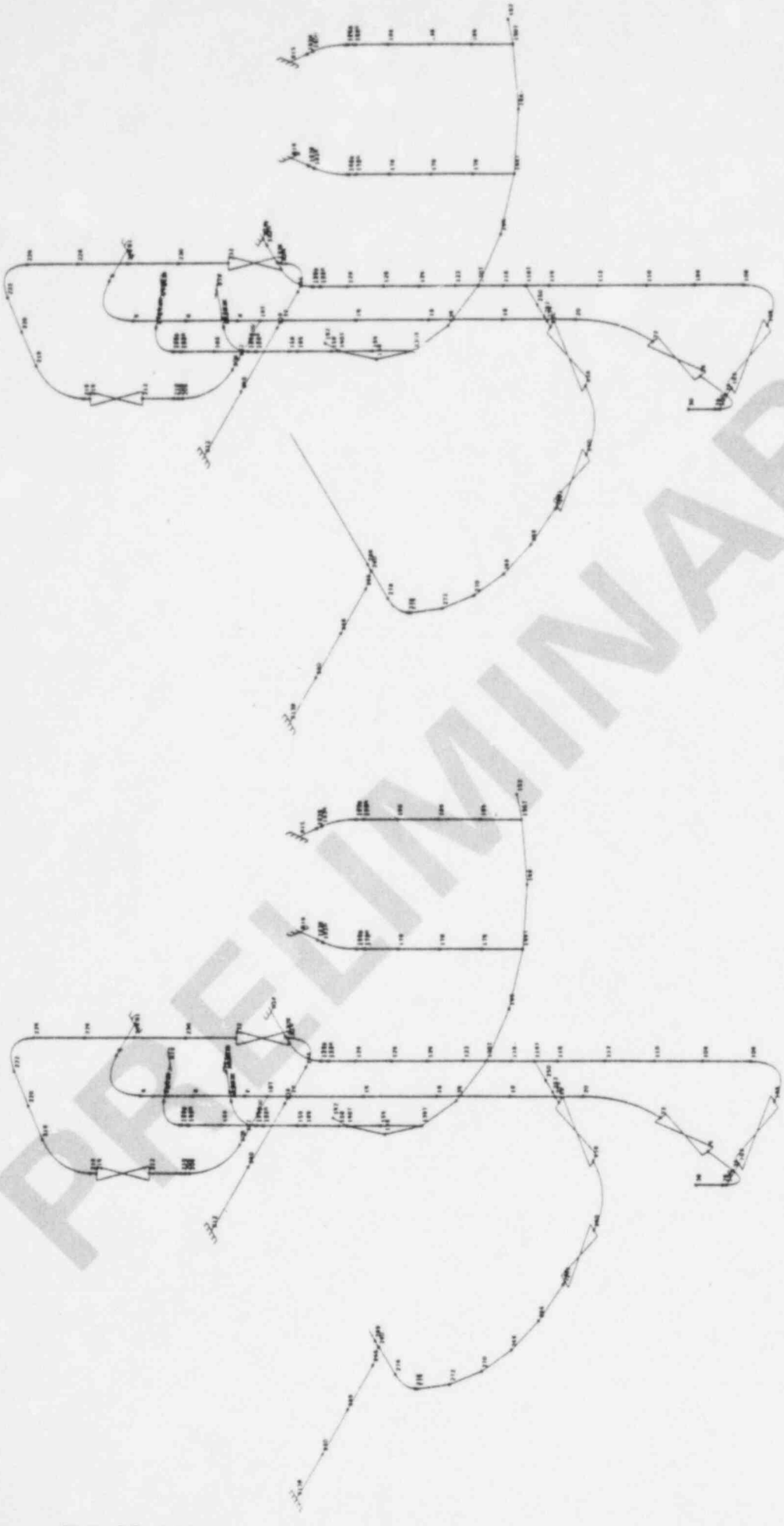

FIGURE 5.15

PIPING MODEL

nutech ENGINEERS

6.0 LEAK-BEFORE-BREAK

6.1 Net Section Collapse

The simplest way to determine the effect of IGSCC on the structural integrity of piping is through the use of a simple "strength of materials" approach to assess the load carrying capacity of a piping section after the cracked portion has been removed. Studies have shown (References 11 and 13) that this approach gives a conservative, lower-bound estimate of the loads which would cause unstable fracture of the cracked section. Typical results of such an analysis are indicated in Figure 6.1 (Reference 11). This figure defines the locus of limiting crack depths and lengths for circumferential cracks which are predicted to cause failure by the net section collapse method. Curves are presented for both typical piping system stresses and stress levels equal to ASME Code limits. Note that a very large percentage of pipe wall can be cracked before reaching these limits (40% to 60% of circumference for through-wall cracks, and 65% to 85% of wall thickness for 360° part-through cracks).

Also shown in Figure 6.1 is a sampling of cracks which have been detected in service, either through UT examination or leakage. In each case there has been a comfortable margin between the size crack that was observed and that which would be predicted to cause failure under service loading conditions. Also, as discussed below, there is still considerable margin between these net section collapse limits and the actual cracks which would cause instability.

6.2 Tearing Modulus Analysis

Elastic-plastic fracture mechanics analyses are presented in Reference 13 which give a more accurate representation of the crack tolerance capacity of stainless steel piping than the net section collapse approach described above. Figures 6.2 and 6.3 graphically depict the results of such an analysis (Reference 13). Through-wall circumferential defects of arc-length equal to 60° through 300° were assumed at various cross sections of a typical BWR Recirculation System. Loads were applied to these sections of sufficient magnitude to produce net section limit load, and the resulting values of tearing modulus were compared to that required to cause unstable fracture (Figure 6.2). Note that in all cases there is

substantial margin, indicating that the net section collapse limits of the previous section are not really failure limits. Figure 6.3 summarizes the results of all such analyses performed for 60° through-wall cracks in terms of margin on tearing modulus for stability. The margin in all cases is substantial.

6.3 Leak Versus Break Flaw Configuration

Of perhaps more significance to the leak-before-break argument is the flaw configuration depicted in Figure 6.4. This configuration addresses the concerns raised by the occurrence of part-through flaws growing, with respect to the pipe circumference, before breaking through the outside surface to cause leakage. Figure 6.4 presents typical size limitations on such flaws based on the conservative, net section collapse method of Section 6.1. Note that very large crack sizes are predicted. Also shown on this figure are typical detectability limits for short through-wall flaws (which are amenable to leak detection) and long part-through flaws (which are amenable to detection by UT). The margins between the detectability limits, and the conservative, net section collapse failure limits are substantial. It is noteworthy that the likelihood of flaws developing which are characterized by the vertical

axis shown in Figure 6.4 (constant depth 360° circumferential cracks) is so remote as to be considered impossible. Material and stress asymmetries always tend to propagate one portion of the crack faster than the bulk of the crack front, which will eventually result in "leak-before-break." This observation is borne out by extensive field experience with BWR IGSCC.

6.4 Axial Cracks

The recent IGSCC occurrences at Monticello and Hatch 1 were predominately short, axial cracks which grew through the wall but remained very short in the axial direction. This behavior is consistent with expectations for axial IGSCC since the presence of a sensitized weld heat-affected zone is necessary, and this heat-affected zone is limited to approximately 0.25 inch on either side of the weld. Since the major loadings in the above net section collapse analysis are bending moments on the cross section due to seismic loadings, and since these loads do not exist in the circumferential direction, the above leak-before-break arguments are even more persuasive for axially oriented cracks. There is no known mechanism for axial cracks to

lengthen before growing through-wall and leaking, and the potential rupture loading on axial cracks is less than that on circumferential cracks.

6.5 Multiple Cracks

Recent analyses performed for EPRI (Reference 21) indicate that the occurrence of multiple cracks in a weld, or cracking in multiple welds in a single piping line do not invalidate the leak-before-break arguments discussed above.

6.6 Crack Detection Capability

IGSCC in BWR piping is detected through two means: non-destructive examination (NDE) and leakage detection. Although neither is perfect, the two means complement one another well. This detection capability combined with the exceptional inherent toughness of stainless steel, results in essentially 100% probability that IGSCC would be detected before it significantly degraded the structural integrity of a BWR piping system.

6.7 Non-Destructive Examination

The primary means of non-destructive examination for IGSCC in BWR piping is ultrasonics. This method has been the subject of considerable research and development in recent years, and significant improvements in its ability to detect IGSCC have been achieved. Nevertheless, recent UT experience at Brunswick 1, Monticello, Hatch 1 and 2, and elsewhere indicate that there is still considerable room for improvement, especially in the ability to distinguish cracks or crack-like indications from innocuous geometric conditions.

Figure 6.4, however, illustrates a significant aspect of UT detection capability with respect to leak-before-break. The types of cracking most likely to go undetected by UT are relatively short circumferential or axial cracks which are most amenable to detection by leakage. Conversely, as part-through cracks lengthen, and thus become more of a concern with respect to leak-before-break, they become readily detectable by UT, and are less likely to be misinterpreted as geometric conditions.

6.8 Leakage Detection

Typical leakage detection capability for BWR reactor coolant system piping is through sump level and drywell activity monitoring. These systems have sensitivities on the order of 1.0 gallon per minute (GPM) of unidentified leakage (i.e., not from known sources such as valve packing or pump seals). Plant technical specification limits typically require investigation/ corrective action at 5.0 GPM unidentified leakage.

Table 6.1 provides a tabulation of typical flaw sizes to cause 5.0 GPM leakage in various size piping (Reference 11).

Also shown in this table are the critical crack lengths for through-wall cracks based on the net section collapse method of analysis discussed above. For conservatism, the leakage values are based on pressure stress only, while the critical crack lengths are based on the sum of all combined loads, including seismic. (Considering other normal operating loads in the leakage analysis would result in higher rates of leakage for a given crack size.) Note that there is considerable

margin between the crack length to produce 5.0 GPM leakage and the critical crack length, and that this margin increases with increasing pipe size.

6.9 Historical Experience

The above theories regarding crack detectability have been borne out by experience. Indeed, of the approximately 400 IGSCC incidents to date in BWR piping, all have been detected by either UT or leakage, and none have even come close to violating the structural integrity of the piping (Reference 21).

NOMINAL PIPE SIZE	CRACK LENGTH FOR 5 GPM LEAK (in.)	CRITICAL CRACK LENGTH ℓ_c (in.)	ℓ/ℓ_c
4" SCH 80	4.50	6.54	0.688
10" SCH 80	4.86	15.95	0.305
24" SCH 80	4.97	35.79	0.139

Table 6.1

EFFECT OF PIPE SIZE ON THE RATIO OF THE CRACK LENGTH FOR 5 GPM LEAK RATE AND THE CRITICAL CRACK LENGTH (ASSUMED STRESS $\sigma = S_m/2$)

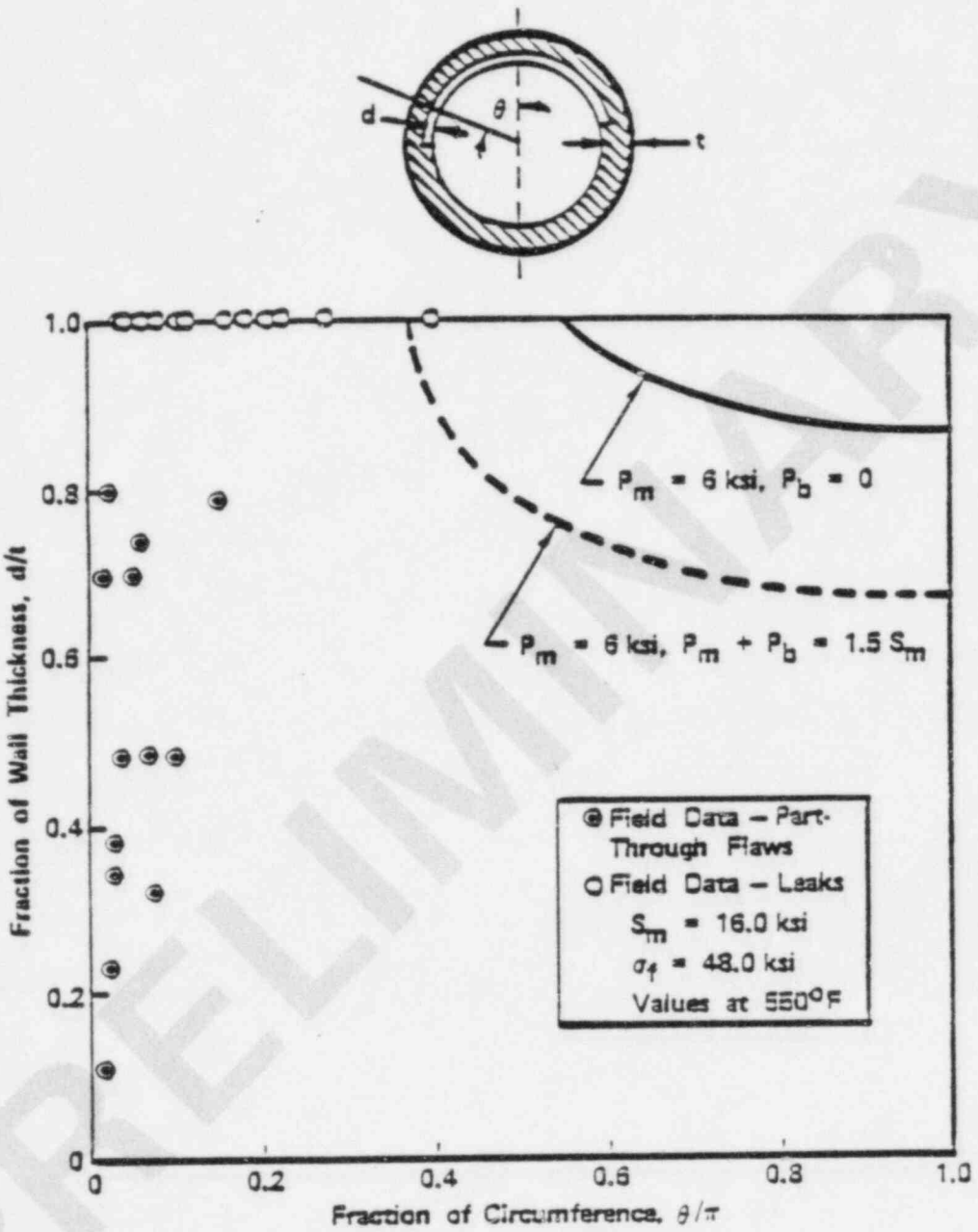

Figure 6.1
TYPICAL RESULT OF NET SECTION COLLAPSE ANALYSIS OF CRACKED STAINLESS STEEL PIPE

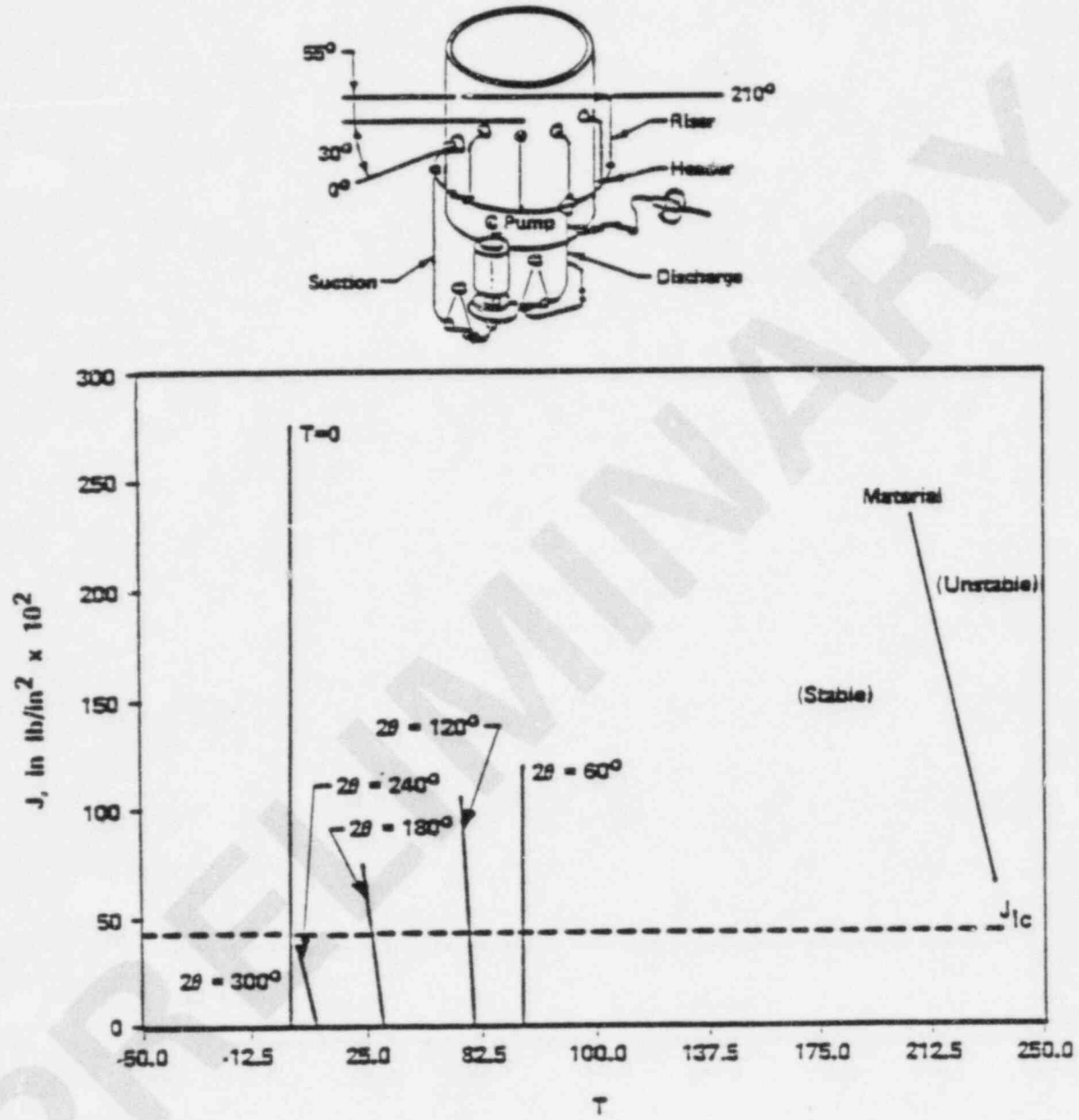

Figure 6.2
STABILITY ANALYSIS FOR BWR RECIRCULATION SYSTEM
(STAINLESS STEEL)

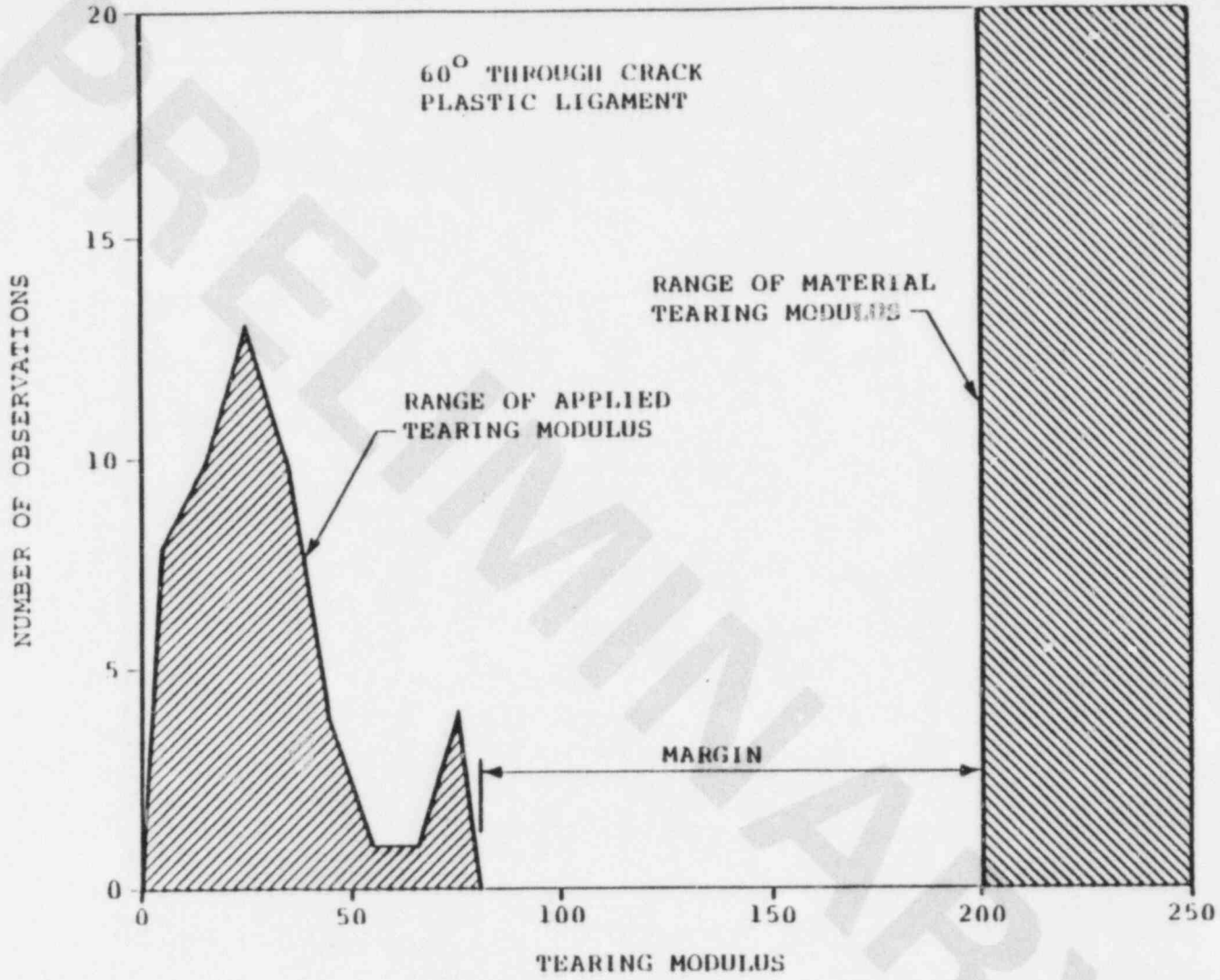

Figure 6.3
SUMMARY OF LEAK BEFORE BREAK ASSESSMENT OF BWR RECIRCULATION SYSTEM

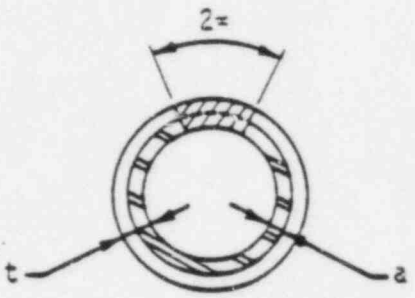

PIPE CROSS SECTION

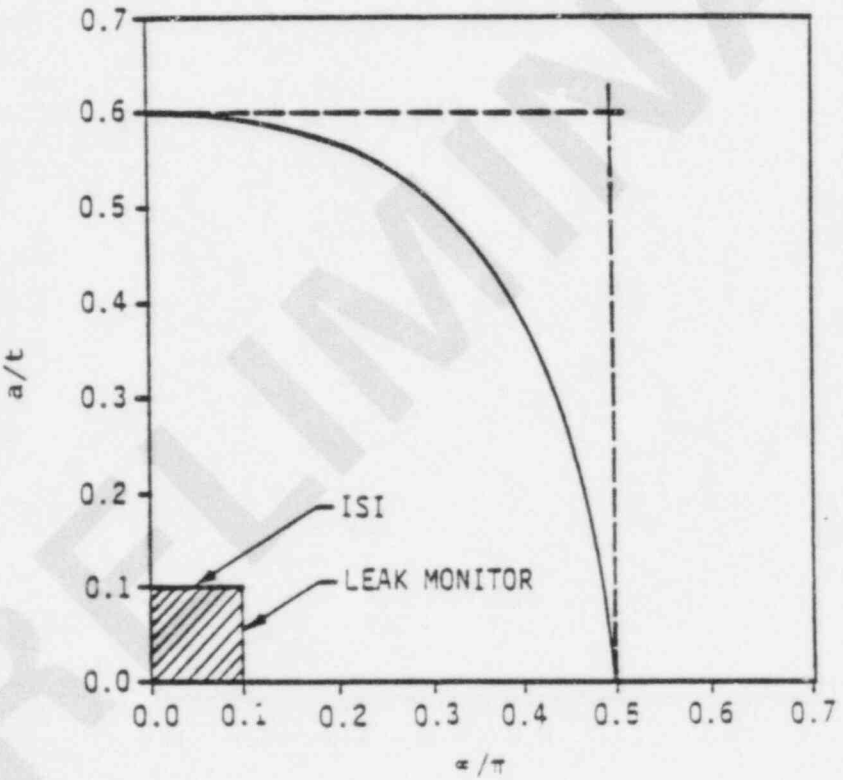

Figure 6.4
TYPICAL PIPE CRACK FAILURE LOCUS FOR COMBINED THROUGH WALL PLUS 360° PART THROUGH CRACK

7.0 SUMMARY AND CONCLUSIONS

The evaluation of the repairs to the Recirculation System reported herein shows that the resulting stress levels are acceptable for all design conditions. The stress levels have been assessed from the standpoint of load capacity of the components, fatigue, and the resistance to crack growth.

Acceptance criteria for the analyses have been established in Section 3.0 of this report which demonstrate that:

1. There is no loss of design safety margin over that provided by the current Code of Construction for Class 1 piping and pressure vessels (ASME Section III).

2. During the design lifetime of each repair, the observed cracks will not grow to the point where the above safety margins would be exceeded.

Analyses have been performed and results are presented which demonstrate that the unrepaired pipe welds and the repaired welds satisfy these criteria by a large margin, and that:

1. The design life of each repair is at least five years.

2. The unrepaired flaws will not grow to an unacceptable size for at least the next fuel cycle.

Furthermore, it is concluded that the recent IGSCC experienced in the Reactor Recirculation System at Hatch 2 does not increase the probability of a design basis pipe rupture at the plant. This conclusion expressly considers the nature of the cracking which has been repaired at Hatch 2, and the likeliood that other similar cracking may have gone undetected. The conclusion is based primarily on the extremely high inherent toughness and ductility of the stainless steel piping material; the tendency of cracks in such piping to grow through-wall and leak before affecting its structural load carrying capacity (which indeed was the case in the defects observed at Hatch 2); and the fact that as cracks lengthen and are less likely to "leak-before-break", they become more amenable to detection by other NDE techniques such as UT and RT.

8.0 REFERENCES

1. ASME Boiler and Pressure Vessel Code Section III, Subsection NB, 1980 Edition.

2. ASME Boiler and Pressure Vessel Code Section XI, Paragraph IWB-3640 (Proposed), "Acceptance Criteria for Austenitic Stainless Steel Piping" (Presented to Section XI Subgroup on Evaluation Standards in November 1982).

3. General Electric Stress Report 22A4264, Revision 0.

4. Bechtel Power Corporation letter to J. E. Charnley, dated May 20, 1983, "E. I. Hatch Nuclear Plant Unit 2, Bechtel Job 6511-034-D3063, Recirculation Line Welding Repair File: A19.3/A21.1 (DCR83-63).

5. General Electric Design Specification 22A1344, Revision 3.

6. ASME Boiler and Pressure Vessel Code Section XI, 1980 Edition with Addenda through Winter 1981.

7. ANSYS Computer Program, Swanson Analysis Systems, Revision 4.

8. Schneider, P.J., "Temperature Response Charts," John Wiley and Sons, 1963.

9. NUTCRAK Computer Program, Revision 0, April 1978, File Number 08.039.0005.

10. EPRI-2423-LD, "Stress Corrosion Cracking of Type 304 Stainess Steel in High Purity Water - a Compilation of Crack Growth Rates," June 1982.

11. EPRI-NP-2472, "The Growth and Stability of Stress Corrosion Cracks in Large-Diameter BWR Piping," July 1982.

12. NUREG-0744, Volume 1 for Comment, "Resolution of the Reactor Materials Toughness Safety Issue."

13. EPRI-NP-2261, "Application of Tearing Modulus Stability Concepts to Nuclear Piping," February 1982.

14. NUTECH Internal Memo, PCR-83-003, "Weld Residual Stress for IGSCC Crack Growth Calculations," March 4, 1983

15. NUTECH Report NSP-81-105, Revision 2, "Design Report for Recirculation Safe End and Elbow Repairs, Monticello Nuclear Generating Plant," December 1982.

16. NUTECH Computer Program PISTAR, Version 2.0, User's Manual, Volume 1, TR-76-002, Revision 4, File Number 08.003.0300.

17. Rybicki, E. F., and McGuire, P. A., "The Effects of Induction Heating Parameters on Controlling Residual Stress in Intermediate Size Pipes," American Society of Mechanical Engineers, 81-PVP-31.

18. Bertossa, D. C., et al, "Techniques to Mitigate BWR Pipe Cracking in Existing Plants (Induction Heating Stress Improvement)" Third Semi-annual Progress Report, November 1979-May 980; NEDC-25146-2, EPRI-RP1394-1, from General Electric to Electric Power Research Institute, May 1980.

19. NUTECH Test Specification for Confirmation Test of Mini Weld Overlay Analytical Model, GPC-07-104, Revision 0, File Number GPC007.0104.

20. NUTECH Testing Corporation, Test Plan and Procedure for Test Confirmation of Mini Weld Overlay Analytical Model, GPC-07-103, Revision 0, File Number GPC007.0103.

21. Presentation by EPRI and BWR Owners Group to U. S. Nuclear Regulatory Commission, "Status of BWR IGSCC Development Program," October 15, 1982.